Mitt. Bayer. Staatsslg. Paläont. hist. Geol.	39	115–149	München, 15. 12. 1999

Stratigraphic Context, Systematic Position and Paleoecology of *Hippotherium sumegense* Kretzoi, 1984 from MN 10 (Late Vallesian of the Pannonian Basin)

By R.L. Bernor[1], T.M. Kaiser[2], L. Kordos[3] and R. S. Scott[4]

With 10 figures and 5 tables

Abstract

Sümeg is a late Vallesian (MN10) karst-fissure locality situated about 60 kilometers north of the western end of Lake Balaton. We update the biochronologic ranking of critical late Miocene (MN9 – MN12) Hungarian localities below based on the stage-of-evolution of murid, cricetid and anomalomyid lineages in order to securely place Sümeg's chronologic position. This diverse vertebrate fauna includes two species of hipparionine horses that we refer here to *Hippotherium sumegense* and "*Hipparion*" sp. small. *Hippotherium sumegense* has short, wide and shallow metapodials and is believed to be a late derived form of the Central European *Hippotherium* s.s. lineage. This species is believed to be the same as the one that appears in the Vallesian Austrian locality of Götzendorf. "*Hipparion*" sp. small is represented by very little material and as such has an indefinite phylogenetic position, but is plausibly related to the small radicle of the *Cremohipparion* lineage, and as such may represent an immigrant from the eastern Mediterranean. Our various analyses suggest that the larger species *Hippotherium sumegense* was a non-cursorial forest denizen with a significant browse component in its diet while "*Hipparion*" sp. small was likely a cursorial form that had a mixed graze-browse diet.

Kurzfassung

Die Fossilienlokalität Sümeg ist eine Karstspaltenfüllung des Oberen Vallesiums (MN10). Sümeg liegt etwa 60 km nördlich des westlichen Ausläufers des Balaton Sees (Ungarn). Um die chronostratigraphische Position von Sümeg zu ermitteln, wird die biostratigraphische Abfolge obermiozäner (MN9–MN12) ungarischer Fundstellen basierend auf Evolutionsstadien der Muriden, Cricetiden and Anomalomyiden herangezogen. Die artenreiche Wirbeltierfauna von Sümeg enthält zwei Arten hipparioniner Pferde, welche hier als *Hippotherium sumegense* and „*Hipparion*" sp. small angesprochen werden. *Hippotherium sumegense* hat kurze, breite und

[1]) R. L. Bernor, College of Medicine, Department of Anatomy, Laboratory of Evolutionary Biology, Howard University, 520 W St. N.W., Washington D.C. 20059, USA; raybernor@compuserve.com

[2]) T. M. Kaiser, Institute and Museum of Zoology, University of Greifswald, D-17489 Greifswald, Germany; kaiser@mail-greifswald.de

[3]) L. Kordos, Museum, Hungarian Geological Institute, Budapest, Hungary; kordosl@compuserve.com

[4]) R. S. Scott, Department of Anthropology, University of Texas at Austin, Austin, Texas 78712-1086, USA; rscott@mail.utexas.edu

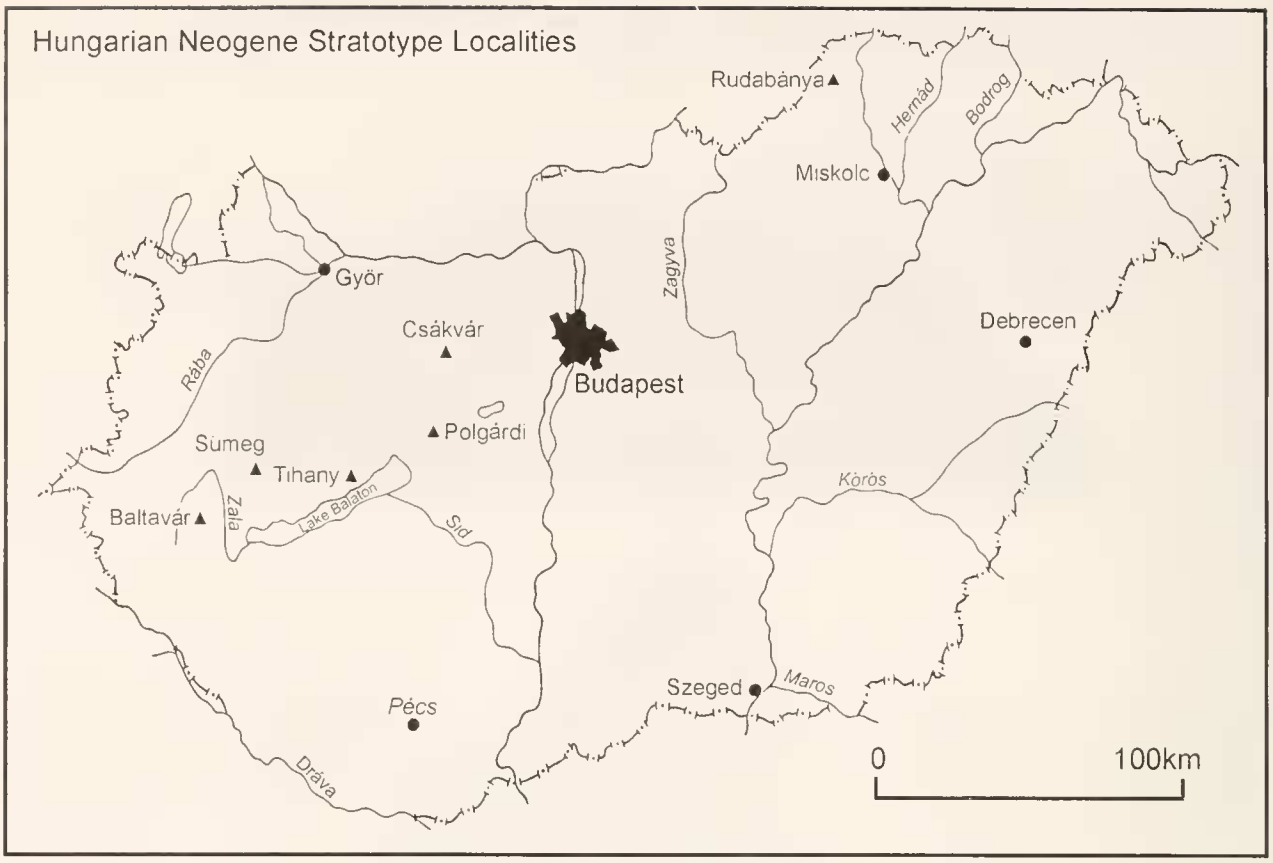

Figure 1: Map of Hungarian Neogene Stratotype Localities.

flache Metapodien, und wird als späte abgeleitete Form der mitteleuropäischen *Hippotherium s.str.* Linie eingestuft. Es ist wahrscheinlich, daß es sich hierbei um die gleiche Art handelt, die an der vallesischen Lokalität Götzendorf (Österreich) auftritt. „*Hipparion*" sp. small ist nur durch sehr wenig Material belegt. Die phylogenetische Stellung dieser Art ist daher schwer zu bestimmen. Die Art ist jedoch am ehesten mit der kleinen Stammgruppe der *Cremohipparion*-Linie in Verbindung zu bringen. Sie dürfte als solche ein Migrant aus dem östlichen Mittelmeerraum sein.

Unsere Analysen weisen darauf hin, daß es sich bei der großwüchsigeren Art *Hippotherium sumegense* um einen non-cursorialen Waldbewohner handelte, dessen Diät größere Anteile weicher Blattnahrung (browse) umfaßte. Die kleinwüchsigere Art „*Hipparion*" sp. small war wahrscheinlich eine cursoriale Form, deren Ernährungsweise eine intermediäre Position zwischen browser (Konzentratselektierer) und grazer (Grasfresser) einnahm.

1 Introduction

The vertebrate locality of Sümeg is situated in the Central Transdanubian Mountains, Hungary, close to the town of Sümeg (N46 57' 55", E17 17' 27"; fig. 1). The locality is situated in the late Cretaceous limestone Gerinc Quarry (Ugod Limestone Formation). Here, late Miocene red clay sediments accumulated in karstic fissures with abundant fossil vertebrates. The fossil vertebrate fauna was first collected by a local fossil hunter, L. Kovacs, and later further exploited by the geologist, J. Fulöp. In 1967, Professor Miklos Kretzoi undertook a major excavation of the Miocene Sümeg vertebrate locality, and his work forms the basis of our

knowledge about the fauna. Subsequent to Kretzoi's excavation, continued mining at the quarry eventually destroyed the fossil-bearing fissures. The geological context of Sümeg has been dealt with previously in Haas et al. (editors, 1984), and the vertebrate fauna has been reported in Hungarian by Kretzoi (1984).

The Sümeg Miocene karst fissure has yielded 61 vertebrate taxa (Kretzoi, 1984) and Kordos (1989) followed studying some groups of rodents. Kretzoi (1969) proposed a new stage, the "Sumegium" which he biochronologically correlated as an intermediate stage between the older "Csakvarium" and younger "Hatvanium" of the Late Pannonian Stage. Kretzoi (1969) characterized the "Sumegium" as: "An assemblage of species most closely related to the Hipparion faunas of southern Europe, Greece, Spain, Italy ("*Pentaglis*", *Progonomys, Rotundomus*, etc) with Asiatic elements (Ovinae) as well as surviving elements from earlier (Central Paratethys) times." Kretzoi & Pecsi (1982) correlated Sümeg with MN12 and Csákvár with MN11 of the European mammal biochronologic system (Mein, 1975, 1979, 1989; Fahlbusch, 1991). Later, Kretzoi (1987) correlated the "Sumegium" with late MN11 or early MN12 (the early late Pannonian), with an age estimation of between 9.2 and 7.5 m.y. Rabaeder (1985) correlated both Sümeg and Csákvár with MN11. Kordos (1992) has correlated Sümeg with MN10 based on the occurrence of *Progonomys,* and Csákvár with MN11 based on the occurrence of *Parapodemus*, and the stage-of-evolution of various anomalomyid species.

1.1 Biochronology of Late Miocene Carpathian Basin Small Mammal-Bearing Localities (MN9-12):

A biochronology of small mammal bearing localities has recently emerged for the Carpathian Basin. Critical to this biochronology are lineages of Muridae, Cricetidae and Anomalomyidae. We provide an updated correlation based on these groups below.

Muridae – *Progonomys* is believed to be absent in the Carpathian Basin during all of MN9 (Rögl et al., 1993; Rögl & Daxner-Höck, 1996). Later, at the locality of Sumegprága (MN10), two species of *Progonomys*, *P. hispanicus* and *P. woelferi*, are found in the absence of the more advanced murid *Parapodemus,* but together with *Pannonicola brevidens* and *Anomalomys petteri* (Kordos, 1992). Kohfidisch and Sümeg (late MN10 or early MN11) both record the co-occurrence of *Progonomys* and *Parapodemus* (Bachmayer & Wilson, 1970; Kretzoi, 1984). The Lake Balaton (Hungary) locality of Tihany (MN11; Kordos et al., in prep.) and Csákvár (Kretzoi, 1954) both record the occurrence of *Parapodemus*, while at the same time they lack *Progonomys*.

Cricetidae – *Democricetodon* and *Eumyarion* last appear in the Carpathian Basin during MN9. The cricetids *Kowalskia* ("*Neocricetodon*"), of the lineage that includes *K. fahlbuschi,* occur in Kohfidisch (Bachmayer & Wilson, 1984). The Sümeg species "*Neocricetodon*" *transdanubicus* (Kretzoi, 1984) has a morphology similar to *K. fahlbuschi* (Kordos, 1992). The Csákvár species "*Neocricetodon*" *schaubi* is more similar to the Tardosbánya taxon *Karstocricetus skofleki* than to *K. fahlbuschi* (Kordos, 1992).

Anomalomyidae. – The Carpathian Basin has yielded abundant remains of Anomalomyidae which reveals the following evolutionary lineage: *A. gaudryi – A. rudabanyensis – A. petteri. Anomalomys gaudryi* first occurs both at the Hungarian locality of Hasznos (Kordos, 1989) and Neudorf Sandberg (Schaub & Zapfe, 1953), both correlated with MN 6. *Anomalomys rudabanyensis* is recognized in the Carpathian Basin from the MN9 locality of Rudabánya (Kordos, 1989) and in Germany from the MN9 locality of Hillenlohe (Germany; Bolliger, 1996). This species would appear to be related to the *A. gaudryi* group as represented at Belchatów A (Poland, MN9, Kowalski, 1994). Some newly discovered and partly unpublished

Vallesian samples of *Anomalomys* have been recorded from Grintzev (Ukraine) and Götzendorf (Austria; ZAPFE et al., 1993) exhibiting a transitional morphology between *A. rudabanyensis* and *A. petteri* (= *Prospalax, Allospalax*). *Anomalomys petteri* is recorded from several late MN10 and MN11 localities of the Carpathian Basin (KORDOS, 1989, BOLLIGER, 1999).

Based on the co-occurrence of *Progonomys, Parapodemus, Kowalskia fahlbuschi* and *Anomalomys petteri*, the Sümeg fauna would appear to correlate closely with Kohfidisch, near the MN10-MN11 transition. The biochronologic sequence of the better known Carpathian Basin MN9-MN12 small mammal-bearing localities is currently believed to be as follows: Rudabánya >Götzendorf >Sumegprága >Kohfidisch >Sümeg >Tihany >Csákvár >Tardosbánya. The Tihany locality has recently become a critical section where rodent biostratigraphy is being coupled with magnetostratigraphy (KORDOS et al., in prep.). Thus far, *Parapodemus* occurs without *Progonomys* at Tihany. Also, *Anomalomys petteri* is present (belonging to the "*Neocricetodon fahlbuschi-Allospalax petteri* Zone"). The Tihany section would appear to record the C4An lower boundary (ca. 9.0 Ma, KORDOS et al., in prep.; STEININGER et al., 1996: Fig. 2.2, pg. 13), as well as the *Congeria balatonica* Zone, giving a maximum age for the lowermost fossil mammal bearing horizons, and the lower boundary for MN11 in the Carpathian Basin. Sümeg would by our correlations be older than the Tihany faunas and have a minimum age of not less than 9.0 Ma giving a congruent result with previous correlations of MN10 being between 9.5 and 9.0 Ma. (STEININGER et al., 1996; RÖGL & DAXNER-HÖCK, 1996). The Sümeg hipparion which we describe herein is very similar to the Götzendorf hipparion and reopens the issue of whether murids do or do not appear in late MN9 of the Pannonian Basin and are controlled in their occurrence by paleoecologic or taphonomic factors (re: BERNOR et al., 1993; RÖGL et al., 1993).

2 Materials and Methods

KRETZOI (1984) reported 18 hipparion teeth and approximately 120, mostly very fragmentary postcranial remains including limb bones, vertebrae and ribs. Table 1 here lists all of the complete material available for our study including the Holotype specimen of "*Hipparion*" *brachypus sumegense* KRETZOI 1984 (MAFIV13242).

We use both continuous and discrete variables here to analyze the hipparion assemblage under consideration. The continuous variables used follow the 1981 American Museum of Natural History Workshop on hipparion research published and illustrated initially by EISENMANN et al. (1988) and again later by BERNOR et al. (1997) who added measurements for some less common postcranial elements and the maxillary and mandibular cheek teeth. These measurements have been used by a number of investigators. We further employ 49 discrete morphological character states of the skull, mandible and dentition to evaluate morphologic variability and evolutionary relationships of the taxa under consideration (re: BERNOR et al., 1996 and BERNOR & ARMOUR-CHELU, 1996; for the most recent update). In a number of studies EISENMANN (re: 1995 for a comprehensive summary) has used log10 ratio diagrams to evaluate differences in hipparion metapodial proportions as a basis for recognizing taxa and interpreting their evolutionary relationships. Here, we also employ ratio diagrams with metapodials to assist in our taxonomic decisions and to better interpret functional and evolutionary trajectories of hipparion locomotor systems. We believe that metapodial morphology may well be subject to a great deal of homoplasy and that it is better to incorporate ratio diagrams into a broader analytical research design that considers other anatomical regions.

In our bivariate analyses we use two Central European populations as standards to which we can compare all other assemblages used in this study: Höwenegg (10.3 Ma [SWISHER, 1996;

Woodburne et al., 1996, 1996a; Bernor et al., 1997]; Hegau, southern Germany) and Eppelsheim (ca. 10.5 Ma [Bernor et al., 1996]; Rheinhessen, Western Germany). Both of these populations are believed to be "biologically uniform", including only a single primitive species, *Hippotherium primigenium*. The Höwenegg population is particularly useful for postcranial comparisons, while Eppelsheim is superior for maxillary and mandibular cheek tooth comparisons because the teeth are most often found without the associated jaws (allowing height measurements), and are more numerous than in the Höwenegg population. Together, these populations allow us to evaluate the size and proportions of the Rudabánya and Sümeg hipparions with a phylogenetic perspective.

2.1 Principal Component Analysis

Principal components analysis (PCA) can be used to identify the major sources of variability in a sample and plots of principal components can be used to identify potential discrete subsets of a sample. Therefore, we have elected to employ principal components analysis of continuous variables for evaluation of the third metacarpal (MCIII) type specimen of "*Hipparion brachypus sumegense*". The continuous variables used follow the 1981 American Museum of Natural History workshop on hipparion research published and illustrated initially by Eisenmann et al. (1988). The six variables used in this analysis were M2, M3, M4, M5, M10, and M12. The raw measurements for each element were all divided by the geometric mean of the measurements for that element (GEOMEAN) and these GEOMEAN corrected measurements were used in the principal components analysis (Jungers et al., 1995). Principal components analysis of the covariance matrix for complete MCIII's was computed using SAS. This analysis included 96 third metacarpals from Sümeg, Rudabánya, Csákvár, Baltavar, Polgardi, Sinap, Esme Akçakoy, Höwenegg, Inzersdorf, Eppelsheim, Inzersdorf, Dorn Dürkheim, Gols, and Xmas Quarry (North America).

While the GEOMEAN correction used for the principal components analysis is designed to correct for the effects of body size, it remains the case that the Höwenegg sample may represent a somewhat larger hipparion species (Bernor et al., in prep.). Thus, an explicit investigation of scaling is in order. With this in mind, body mass estimates were made for the sample of MCIII's included in our principal component analysis whenever possible. These estimates were derived using the regression formulae of K. Scott (1990). These equations were used to estimate body mass based on M3 (mid-shaft breadth), M4 (mid-shaft depth), M5 (proximal articular surface breadth), M6 (proximal articular surface depth), and M10 (breadth across distal supra-articular tuberosities). The mean of these estimates was taken as an overall estimate of body mass. Thus, estimated body mass is the mean of estimates based on non-length measurements following both the formulae and methodology of K. Scott (1990). Since M6 was included in the determination of estimated body mass and was not available for all specimens in our PCA, only 90 of these specimens have associated estimated body masses. We regard this estimate as useful for making body mass comparisons between MCIII specimens but as yet estimates based on MCIII's are not strictly comparable to estimates similarly derived for MTIII's. Least squares regressions between estimated body mass and logged measurements for the complete MCIII sample and the Höwenegg sample alone were undertaken to identify potential scaling relationships between variables. These regressions also allowed the computation of residuals for key variables as an alternative method of size correction.

2.2 Microwear analysis and analysis of macroscopic occlusal wear features

Light microscopic investigation of occlusal surfaces was carried out with an Olympus SZH10 stereo microscope. Specimens were coated with ammonium chloride (NH_4CL). Black and white photographs were taken with a Kontron 3012 (Carl Zeiss Jena) high resolution digital camera at 4500x3200 pix. SEM investigation has been carried out using replica technique as described. After cleaning specimens with acetone and varnish remover (Zip-Strip, Star Bronce Company, Alliance, Box 2206, Ohio 44601–0206) (re: HAYEK, et al. 1992), molds were taken using Provil novo Monophase (Heraeus Kulzer) polysiloxane dental molding material. Replicas are reversed using epoxy resin Injektionsharz EP (Recki-Chemiewerkstoff Co, D-44629 Herne). The replicas were mounted on Al-stabs, using conductive-C cement (Neubauer Chemikalien, D-48031 Münster) and sputter coated with 25µ Gold employing an Edwards Sputter Coater S15 0B. Investigation was carried out with a Zeiss DSM 940A Scanning Electron Microscope at 4–5kV. Images were taken on Kodak TMAX 100.

Microwear analysis was undertaken using a qualitative approach. Following HAYEK et al. (1992), SEM micrographs were taken of the occlusal surface of the ectoloph just labial to the paracone. Photographs were taken perpendicular to the occlusal surface with a standard magnification of 500 X. Due to the small number of Sümeg specimens, our sample could not be restricted to upper M2 as advocated by HAYEK et al. (1992). We include all Sümeg upper and lower cheek teeth in this study (Tables 2–3) and have selected a sample of upper cheek teeth for comparison with hipparion specimens from Eppelsheim and Rudabánya. The overall appearance of the microwear features is interpreted in terms of dietary reconstruction following HAYEK et al. (1992) and SOLOUNIAS & HAYEK (1993). When the ratio of length to width is less than, or about equal to four it is termed a pit. When the length to width ratio is more than four it is termed a scratch (TEAFORD & ROBINSON, 1987 and SOULONIAS et al., 1988).

2.3 Abbreviations and Conventions

AMNH – American Museum of Natural History, New York
HLMD – Hessisches Landesmuseum, Darmstadt
MAFI – Hungarian Geological Institute Museum (MAFIV indicates vertebrate collection of the MAFI).
NHMW – Naturhistorisches Museum, Wien
SENK – Senckenbergmuseum Frankfurt
SMNK – Staatliches Museum für Naturkunde, Karlsruhe.

The taxon *Hipparion* has been applied in a variety of ways by different authors. We follow definitions provided in BERNOR et al. (1996, 1997).

2.4. Measurements

Measurements are in millimeters (mm) (all measurements as defined by EISENMANN et al., 1988 and BERNOR et al., 1997 and rounded to 0.1 mm).

tx refers to maxillary teeth

tm refers to mandibular teeth

Table 1: Measurements on Sümeg hipparions. MAFI NO. = Hungarian Geological Institute Museum specimen accession number; NO = specimen number of teeth provisionally assigned in text for discriminating individuals; SPECIES = Hsum refers to *Hippotherium sumegense,* Hipsm to Hipparion" sp (small). BONE = skeletal element (tx = maxillary tooth, tm = mandibular tooth, ast = astragalus, mciii = metacarpal III; mtiii = metatarsal III; radii = radius, tibia = tibia;), S = side (rt = right, lt = left), M = measurement number. Measurements follow EISENMANN et al. (1988) and BERNOR et al. (1997).

MAFI NO.	NO	SPECIES	BONE	S	M1	M2	M3	M4	M5	M6	M7	M8	M9	M10	M11	M12	M13	M14
MAFIV13246A		Hsum	ast	1	56.1	57.2	29.2	58.6	45.6	31.2	48.9							
MAFIV13246B		Hsum	ast	1	51.9	52.6	26.5	52.7	39.6	29.0	42.9							
MAFIV13246C		Hsum	ast	2			28.6	59.3	45.1	29.6	42.7							
MAFIV13246D		Hsum	ast	2	49.8		28.2	54.0	43.7	32.7	39.0							
MAFIV13246E		Hsum	ast	1			24.6											
MAFIV13242		Hsum	mciii	2	193.1	187.2	29.3	20.2	37.7	25.7	32.9	11.8	5.2	36.8	33.9	25.9	22.6	24.8
MAFIV13244A		Hsum	mciii	1			30.9	22.2	40.8	26.7	33.7	12.1	4.0					
MAFIV13244B		Hsum	mciii	2			28.7	22.2	39.6	27.9	33.7	11.4	5.1					
MAFIV13244C		Hsum	mciii	1					35.8	27.4	30.3	12.0	4.8					
MAFIV13244D		Hsum	mciii	2					37.1	25.9	32.5	10.2	5.3					
MAFIV13244E		Hsum	mciii	2			27.3	18.7	36.9	25.3	31.7	10.1	6.1					
MAFIV13244F		Hsum	mciii	1			30.0	19.3	35.5	26.4	31.7	10.0	4.2					
MAFIV13244G		Hipsm	mciii	1					31.4	21.8	28.4	9.4	4.8					
MAFIV13245B		Hsum	mciii	1			28.6	20.0	36.0	25.7	31.9	11.3	6.3					
MAFIV13245C		Hsum	mciii	2			28.7	21.1						35.5	34.0	26.3	22.6	24.6
MAFIV13245D		Hsum	mciii	1										39.3	37.7	28.4	24.0	25.5
MAFIV13245E		Hsum	mciii	1			30.5	20.9		27.7			5.0					
MAFIV13245F		Hsum	mciii	1										34.8	33.1	27.7	23.6	25.4
MAFIV13245G		Hsum	mciii	2										37.9	34.4	22.2	23.4	25.3
MAFIV13245H		Hsum	mciii	2										35.5	34.0	24.7	21.6	24.0
MAFIV13245I		Hsum	mciii	2											35.1	26.0	22.1	23.1
MAFIV13245J		Hsum	mciii	1										37.0	34.1	26.7	23.9	25.5
MAFIV13245K		Hsum	mciii	2										38.4	37.0	28.5	24.3	25.7
MAFIV13245L		Hsum	mciii	2										38.8	37.3	27.5	23.3	26.2
MAFIV13244H		Hsum	mtiii	1						32.5								
MAFIV13244I		Hsum	mtiii	1			31.0	28.0	41.7	34.8	38.6	10.1	6.3					
MAFIV13245A		Hsum	mtiii	2										38.6	36.2	29.4	23.4	26.7
MAFIV13245M		Hsum	mtiii	2			29.8	26.8						37.2		28.6	25.0	
MAFIV13245N		Hsum	mtiii	1										36.4	34.2	30.3	24.5	27.0
MAFIV13245O		Hsum	mtiii	1										38.0	36.3	30.8	24.9	28.4
MAFIV13259		Hsum	radii	2					59.7	33.9	66.0							
MAFIV113259A		Hsum	tibia	1			44.2	28.7			64.9	41.8						
MAFIV13259B		Hsum	tibia	1			44.5	28.2			60.9	39.9						
MAFIV13257		Hsum	tmdP2	1	31.9	28.9	10.4	8.4	12.9	9.4	13.7	7.3	8.3	14.3				
MAFIV13266E	5b	Hipsm	tmM1	2	21.9	21.2	14.4	6.9	10.3	12.0	14.1	10.6	10.0	40.5				
MAFIV13266F	3b	Hsum	tmM1	1	25	22.1	14.6	8.3	10.6	11.8	14.1	10.7	10.3	43.4				
MAFIV13266G	3c	Hsum	tmM2	1	26.6	22.2	13.4	8.7	11.2	10.9	12.0	9.2	8.9	43.4				
MAFIV13267C		Hsum	tmM3	2	27.3	27.6	9.8	5.0	7.2	11.8	11.5	10.3	9.3	17.6				
MAFIV13266A	1a	Hsum	tmP2	2	29.4		11.9	7.9	13.5	11.6	14.2	10.8	13.5	29.7				
MAFIV13266H	6	Hipsm	tmP2	1			11.9	6.9	11.4	12.9		11.4	13.2					
MAFIV13266B	1b	Hsum	tmP3	2	26.5	23.3	14.3	8.2	13.3	14.4	14.4	13.8	13.8	40.7				
MAFIV13267B		Hsum	tmP3	2	21.6	21.2	12.7	7.1	9.4	15.1	15.6	13.0	12.1	18.4				
MAFIV13266C	1c	Hsum	tmP4	2	27	23.6	12.7	8.4	12.9	13.0	15.7	11.5	11.9	46.8				
MAFIV13266D	3a	Hsum	tmP4	1	27.9	23.7	14.8	8.3	13.7	14.0	14.3	12.8	14.5	38.4				
MAFIV13266G	5a	Hipsm	tmP4	2	22.5	20.9	12.1	6.6	10.3	13.8	12.4	11.9	10.1	29.9				
MAFIV13267A		Hsum	tmP4	1	26.5	22.9	13.0	7.4	13.0	14.0	15.0	11.0	11.7	48.8				
MAFIV13266C		Hsum	txM1	1	21.2	19.3			28.6	1	8	5	3	6.6	4.5			
MAFIV13266D	7	Hipsm	txM1	1	22.1	18.7	22.3	21.4	30.8	3	8	5	2	5.3	3.4			
MAFIV13266E	4	Hsum	txM2	2	22.9	20.9	23.2	22.9	34.4	7	5	5	5	6.5	4.3			
MAFIV13266A	2a	Hsum	txP2	1		29.4	22.0	20.8	23.7	2	6	6	3	6.9	4.1			
MAFIV13267A		Hsum	txP2	2	31.3	30.8	23.3	22.0	27.7	4	4	7	3	7.3	4.6			
MAFIV13267B		Hsum	txP2	1			23.0	23.9	30.1	5	8	8	3	5.6	4.1			
MAFIV13266D	2b	Hsum	txP3	1	24.4	22.2	23.8	23.5	29.0	6	7	6	2	6.7	4.2			
MAFIV13267C		Hsum	txP3	1	24.8	20.8	23.4	22.8	32.0	2	2	4	2	7.3	4.2			
MAFIV13266B	2c	Hsum	txP4	1	22.2	20.6	21.9	22.1	32.9	4	8	5	1	7.2	5.3			

2.5. Anatomical Descriptions

The osteological nomenclature has been adapted from NICKEL et al. (1986). GETTY (1982) was also consulted for morphological identification and comparison. Hipparion monographs by GROMOVA (1952) and GABUNIA (1959) were cited after the French translations.

Cheek tooth ontogenetic stages are: 0 = unerupted; 1 = just erupted, early wear, juvenile; 2 = tooth with entire occlusal face worn but not yet to the middle of the tooth; 3 = middle stage-of-wear; 4 = very worn tooth.

Character state tables have the following abbreviations:

C refers to character state by number as given in the Legend for tables 1 and 2
MAFI NO. = HGI Museum accession number
NO. = number provisionally assigned here to clarify likely individual association.
SPECIES = Hsum refers to *Hippotherium sumegense,* Hipsm to "Hipparion" sp (small).
BONE = skeletal element (tx = maxillary tooth, tm = mandibular tooth).
S = side (rt = right, lt = left).

The bivariate plots are keyed to specific localities by letters. We use RÖGL & DAXNER-HÖCK (1996), STEININGER et al. (1996), SWISHER (1996), and WOODBURNE et al. (1996, 1996a) for our age estimates. The localities referred to in the bivariate plots that follow include:

A = Altmansdorf (MN9, Pannonian D-E, ca. 10.5+ Ma), Austria
C = Csákvár (MN11), Hungary
D = Dorn Dürkheim (MN11), Germany
E = Eppelsheim (MN9, ca. 10.5 Ma), Germany
G = Gaiselberg (MN9, Pannonian C, ca. 11 Ma), Austria
H = Höwenegg (MN9, 10.3 Ma), Germany
I = Inzersdorf (MN9, Pannonian D-E, ca. 10.5 Ma), Austria
L = Gols (MN10), Austria
P = Prottes (MN10), Austria
R = Rudabánya (MN9, ca. 10 Ma), Austria
S = Sümeg (MN11), Hungary
T = Sinap (MN9-10; 10.8-9 Ma), Turkey [only 2 critical specimens included herein]

3 Distribution of Morphological Characters

3.1 Discrete Characters of the Skull

3.1.1 Maxillary Cheek Teeth

Table 2 gives the character state distribution of maxillary teeth from the Sümeg sample. BERNOR & FRANZEN (1997; Dorn Dürkheim) and BERNOR et al. (1997; Höwenegg) made detailed studies of character state distribution of all teeth and found degrees of variation depending both on the tooth's stage-of-wear and the particular character state in question. The Dorn Dürkheim (DD) sample showed a higher degree of variability than the Höwenegg (Hö) population in both discrete and continuous variables. This is probably due to some degree of time averaging in the DD sample versus the geologically "nearly instantaneous" accumulation of the Hö sample (re: WOODBURNE et al., 1996a). There is a small sample of maxillary cheek teeth from Sümeg that has been evaluated using our character state scoring below, and compared to the primitive condition for Central European *Hippotherium primigenium* (re: BERNOR et al., 1997).

Character 17 is the curvature of the maxillary cheek teeth. As in *Hippotherium primigenium*, curvature is moderate (state = B).

Character 18 is maximum cheek tooth crown height. As for all members of the *Hippotherium* lineage, maximum crown height of this sample was between 40 and 60 mm (state = C).

Character 19 is maxillary cheek tooth fossette ornamentation. As in *Hippotherium primigenium*, the enamel plications are complex (state = A). Moreover, in this sample there is a very strongly developed bucco-lingual groove across the mesostyle-protocone. This groove creates high sharp crests along the midline of the prefossette and postfossette. We provide further interpretations to this below in the macroscopic occlusal wear portion of our manuscript.

Character 20 is the morphology of the posterior wall of the postfossette. Whereas more primitive species of North American *Cormohipparion* and Turkish *Cormohipparion* have a moderate incidence of fusion of the postfossette with the posterior wall of the tooth, it is less marked in *Hippotherium primigenium* and entirely absent in the Sümeg sample (state B).

Character 21 is pli caballin morphology. In *Hippotherium primigenium* state A, double pli caballins, is a fairly consistent state in middle 1/2 wear. The Sümeg sample is derived in having some incidence of a single pli (state = B).

Character 22 is the morphology of the hypoglyph. In *Hippotherium primigenium* the prevailing state is B, deeply incised and infrequently encircled hypocone. In the Sümeg sample the hypoglyph in all but one individual is state B; this other individual expresses a slightly less incised hypoglyph (state = C).

Character 23 is protocone shape. This character can vary tremendously in all hipparion populations. In the Sümeg population most protocones are oval (= C), but some lingual flattening (= E) occurs in two individuals.

Character 24 is isolation of the protocone. Rarely, and almost only in late wear, the protocone forms an open connection with the protoloph (state A). In the Sümeg population the protocone is always isolated from the protoloph (= B).

Character 25 is the occurrence of a protoconal spur, clearly a primitive character in hipparions that occurs with modest frequency in *Hippotherium primigenium* (Bernor & Franzen, 1997). In the Sümeg population the protoconal spur is absent in all specimens (= C) except a single individual (= B) where it is very reduced.

Character 26 is premolar protocone/hypocone alignment. In Höwenegg *Hippotherium primigenium* this state is always B, protocone more lingually placed than the hypocone; it is so in the Sümeg population.

Character 27 is molar protocone/hypocone alignment. State A, anteroposterior alignment, occurs more frequently in molars than in the premolars. Amongst molars, it occurs most frequently in M3 due to the labiolingual compression of its crown. In the one M1 and one M2 of the Sümeg sample, the protocone is placed lingual to the hypoglyph (= B).

3.1.2 Mandibular Cheek Teeth

Table 3 provides the character state distribution of mandibular cheek teeth. Bernor et al.'s (1997) and Bernor & Franzen's (1997) study of the Höwenegg and Dorn Dürkheim populations of *Hippotherium primigenium* revealed that mandibular cheek tooth character states were more variable than the maxillary ones in these populations. Yet, in middle stage-of-wear there is reasonable stability for many mandibular cheek tooth characters. We have no other comparable data on mandibular cheek teeth for any Old World hipparion other than those from the German late Miocene.

Table 2: Character state distribution of Sümeg maxillary cheek teeth. MAFI NO. = Hungarian Geological Institute Museum specimen accession number; NO = specimen number of teeth provisionally assigned in text for discriminating individuals; SPECIES = Hsum refers to *Hippotherium sumegense*, Hipsm to Hipparion" sp (small). BONE = skeletal element (tx = maxillary tooth). For character state identification (C17-C27) see Legend.

MAFI NO.	NO	SPECIES	BONE	S	A	C17	C18	C19	C20	C21	C22	C23	C24	C25	C26	C2
MAFIV13266D	7	Hipsm	txM1	rt	3	B	C	A	B	B	B	E	B	C		B
MAFIV13266E	4	Hsum	txM2	lt	3	B	C	A	B	B	B	CE	B	C		B
MAFIV13266A	2a	Hsum	txP2	rt	3+	B	B	A	B	A	C	C	B	B	B	
MAFIV13266D	2b	Hsum	txP3	rt	3	B	C	A	B	C	B	C	B	C	B	
MAFIV13266B	2c	Hsum	txP4	rt	3+	B	C	A	B	A	B	C	B	C	B-	

Character 32 is the morphology of the premolar metaconid. There are two different states in the Sümeg sample: one which is a simple rounded morphology (= A) and another which is more elongate and sub-square/round shape (= B/AE); the latter state is derived compared to *Hippotherium primigenium*.

Character 33 is molar metaconid morphology. There is a single m1 (specimen #5b) which conforms closely to the simple rounded morphology (= A) of the premolar metaconids and, in fact may be of the same individual (specimens #5a and #5b; Tables 1 and 3). Two additional premolar specimens (#3b and #3c) have elongated and sub-rounded metaconids (= BA).

Character 34 is premolar metastylid morphology. Again, there are two prevailing states in the Sümeg sample: subsquare/rounded (= AE; smaller form) and irregular shape (= D; larger form). State AE is found in Central European *Hippotherium primigenium*, while state D is derived and reported in the Götzendorf (Vienna Basin) hipparion (Bernor et al., 1993; Rögl et al., 1993).

Character 35 is occurrence of the premolar metastylid spur. *Hippotherium primigenium* occasionally expresses the metastylid spur (state A), with the highest frequency being on p2 (Bernor & Franzen, 1997; Bernor et al., 1997). The Sümeg sample expresses state A strongly in the larger form, but lacks it altogether in the small form.

Character 36 is molar metastylid morphology. There is one small individual m1 (specimen #5b), and this specimen exhibits the angular/square morphology (= CE) typically found in *H. primigenium*. This morphology is also found in the two specimens belonging to the large form (#3b and #3c).

Character 37 is the occurrence of molar metastylid spurs. There is an m1 in our sample (specimen #5b) that belongs to the small morph, and this specimen lacks the metastylid spur (= B). This is an advanced character for Old World hipparion. Two molars belonging to the large morph (specimens #3b and #3c) have metastylid spurs (state A).

Character 38 is premolar ectoflexid morphology. Rarely, *Hippotherium primigenium* exhibits state B whereby the ectoflexid projects between metaconid and metastylid, and most usually this is in p2. The entire Sümeg sample exhibits state A.

Character 39 is molar ectoflexid morphology. The usual state is B for molars and this is the state exhibited in the Sümeg sample.

Character 40 is pli caballinid morphology. The prevailing state in the Sümeg population is B, single or rudimentary, with three individuals exhibiting state C (absent).

Character 41 is protostylid morphology. The Sümeg sample is derived in mostly exhibiting reduced, small pointed projection limited to the lower aspect of the crown (= F). In one worn

Table 3: Character state distribution of Sümeg mandibular cheek teeth. MAFI NO. = Hungarian Geological Institute Museum specimen accession number; NO = specimen number of teeth provisionally assigned in text for discriminating individuals; SPECIES = Hsum refers to *Hippotherium sumegense*, Hipsm to Hipparion" sp (small). BONE = skeletal element (tx = maxillary tooth). For character state identification (C32-C49) see Legend.

MAFI NO.	NO	SPECIES	BONE	S	A	C32	C33	C34	C35	C36	C37	C38	C39	C40	C41	C42	C43	C44	C45	C46	C47	C48	C49
MAFIV13266F	3b	Hsum	tmM1	rt			BA			CE	A		B	C	F	A	B		B	B-	B-	A	A
MAFIV13266E	5b	Hipsm	tmM1	rt	4		A			CE	B		B	C	A	B	B		D	A	A	A	A
MAFIV13266G	3c	Hsum	tmM2	rt			BA			CE	A		B	C	F	A	B		B	B	B-	A	B-
MAFIV13266H	6	Hipsm	tmP2	rt		A		AE	B			A		B-			B	B		A	B-	A	A
MAFIV13266A	1a	Hsum	tmP2	lt	3	BE		D	A			A		B	B		B	C+		A	B	A	B
MAFIV13266B	1b	Hsum	tmP3	lt	3+	BA		D	A-			A		B	F	A	B	C+		B-	B-	A	B-
MAFIV13266C	1c	Hsum	tmP4	lt	3+	BA		D	B			A		B	F	A	B	C+		B	B	A	B-
MAFIV13266D	3a	Hsum	tmP4	lt	3	BA		D	A			A		B	F	A	B	C+		A	B	A	B-
MAFIV13266G	5a	Hipsm	tmP4	lt	3	A		AE	B			A		B	F	B	B	B		B	A	A	A

individual (specimen #5b) it is expressed as an enclosed ring (= A) and on another individual (specimen #1a) it is absent (= B).

Character 42 is protostylid orientation. In five individuals protostylid courses obliquely to the anterior surface of the tooth (= A), while in two others it is less oblique coursing rising on the corner defined by the mesial and labial walls of the tooth (= B). The former character is primitive for Old World hipparions, while the latter is derived.

Character 43 is ectostylid morphology. Eurasian hipparions generally lack ectostylids in the permanent dentition. In fact, they have only been found rarely in very worn Dinotheriensande cheek teeth. Ectostylids occur in the adult cheek teeth of latest Miocene – Pleistocene African hipparions and become a significant feature of their evolution (Bernor & Armour-Chelu, 1996; in press). All specimens in the Sümeg sample lack an ectostylid (=B).

Character 44 is premolar linguaflexid morphology. In four specimens the linguaflexid is derived, being very broad, shallow (= C+) and frequently interrupted by a prominent metastylid spur. Two individuals (specimens #5a and #6) exhibit the primitive condition of being shallow and V-shaped (as is common in *H. primigenium*).

Character 45 is molar linguaflexid morphology. There is one individual expressing state D; deep, broad U-shape, and two individuals exhibiting a V-shaped morphology (= B).

Character 46 is preflexid morphology. Both complex (= B) and simple (= A) morphologies are expressed in this sample.

Character 47 is postflexid morphology. Both complex (= B) and simple (= A) morphologies are expressed in this sample.

Character 48 is postflexid morphology at the metaconid/metastylid junction. As in all but one species of advanced Old World hipparion, state A does not bend sharply lingually.

Character 49 is protoconid enamel band morphology. The primitive condition for Old World hipparions is state A (rounded) with state B (flattened) being advanced. This sample includes five individuals exhibiting slight flattening of the protoconid enamel band. However, this is not accompanied by band lengthening which is common in more advanced members of the "*Sivalhippus*" Complex (Bernor et al., 1989, 1996).

3.2 Statistical Analysis of Continuous Variables of the Skull

3.2.1 Cheek Teeth

All cheek tooth comparisons use the Eppelsheim *Hippotherium primigenium* sample as the standard for calculating 95% confidence ellipses.

Maxillary

While we analysed several bivariate dimensions for all the maxillary cheek teeth, we found the results to be largely redundant between tooth classes. We have chosen to use P2 and P4 to compare sizes (M3 = occlusal width, M1= occlusal length) between Sümeg and other Central European and Turkish samples here. There is only a single P2 and a single P4 in our sample, and both of these fall in the lower portion of the Eppelsheim ellipse (Figures 2a, 2b). Referral to these two plots reveal that most of our sample falls within these two ellipses, with specimens from Dorn Dürkheim (D; several specimens), Csákvár (C), Gaiselberg (G), Rudabánya (R) and Götzendorf (Z) being found outside the ellipse.

Mandibular

We have made a similar analysis of mandibular p2's. Figures 3a-b are plots of M8 (maximum occlusal width across metaconid-protoconid enamel bands) versus M1 (occlusal length) on p2 and p4, respectively. All except a single Sümeg individual (5a) fall within these two ellipses. On morphological (character state) grounds that same individual is identified here as being referable to Hipsm and distinctly different from the predominate Sümeg hipparion. Again, Dorn Dürkheim (D) has several individuals outside the ellipse, with particularly lower values for p2 length. The Austrian Turolian locality of Gols (L) likewise has an individual with reduced width measurements.

3.3 Proposed Association of Elements in Cheek Tooth Dentitions

Based on comparable cheek tooth crown height, state of preservation, fit of interproximal wear facets, and commonality of character states (Tabs. 2, 3) we believe that the 14 cheek teeth listed in Table 2–3 represent a maximum number of 7 individuals. Teeth believed to be associated and belonging to a single individual include: a left tmP2–tmP4 (specimen numbers 1a, 1b, 1c); a right tmP4–tmM2 (specimen numbers 3a, 3b, 3c), a left tmP4–tmM1 (specimen numbers 5a, 5b) and a right txP2–txP4 (specimen numbers 2a, 2b, 2c). The remaining specimens are believed to be isolated specimens each belonging to a single individual.

3.4 Postcrania

3.4.1 Bivariate Plots for the Anterior Limb

All postcranial bivariate plots use the Höwenegg sample for calculating 95% ellipses. Metacarpal III is the only element from the forelimb that we analyze. Figures 4a–c plot

Figure 2: a. Maxillary P2, M3 (occlusal width) versus M1 (occlusal length); b. Maxillary P4, M3 (occlusal width) versus M1 (occlusal length). These and succeeding bivariate plots of various measurements (see legend and tables). Ellipse circumscribes 95% confidence limits. Symbols refer to the following localities: A = Altmansdorf, Austria; C = Csákvár, Hungary; D = Dorn Dürkheim, Germany; E = Eppelsheim, Germany; G = Gaiselberg, Austria; H = Höwenegg, Germany; I = Inzersdorf, Austria; L = Gols, Austria; P = Prottes, Austria; R = Rudabánya, Hungary; S = T = Sinap, Turkey.

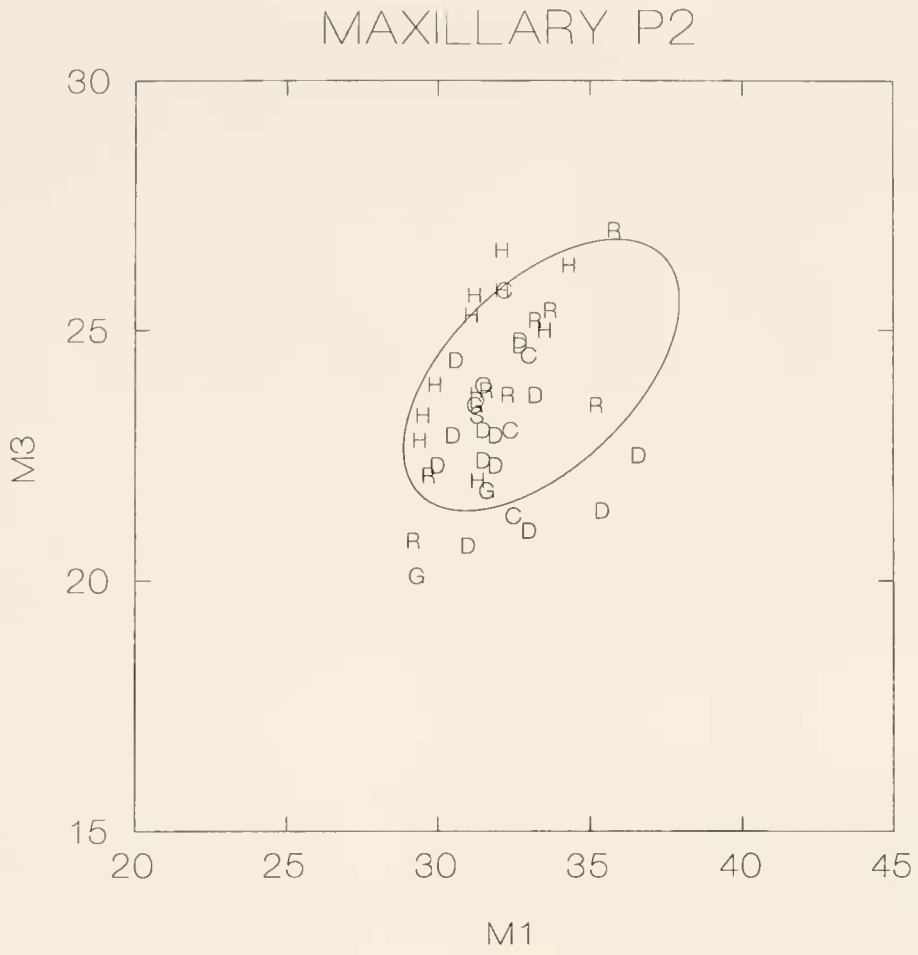
MAXILLARY P2
M3
M1
30
25
20
15
20
25
30
35
40
45

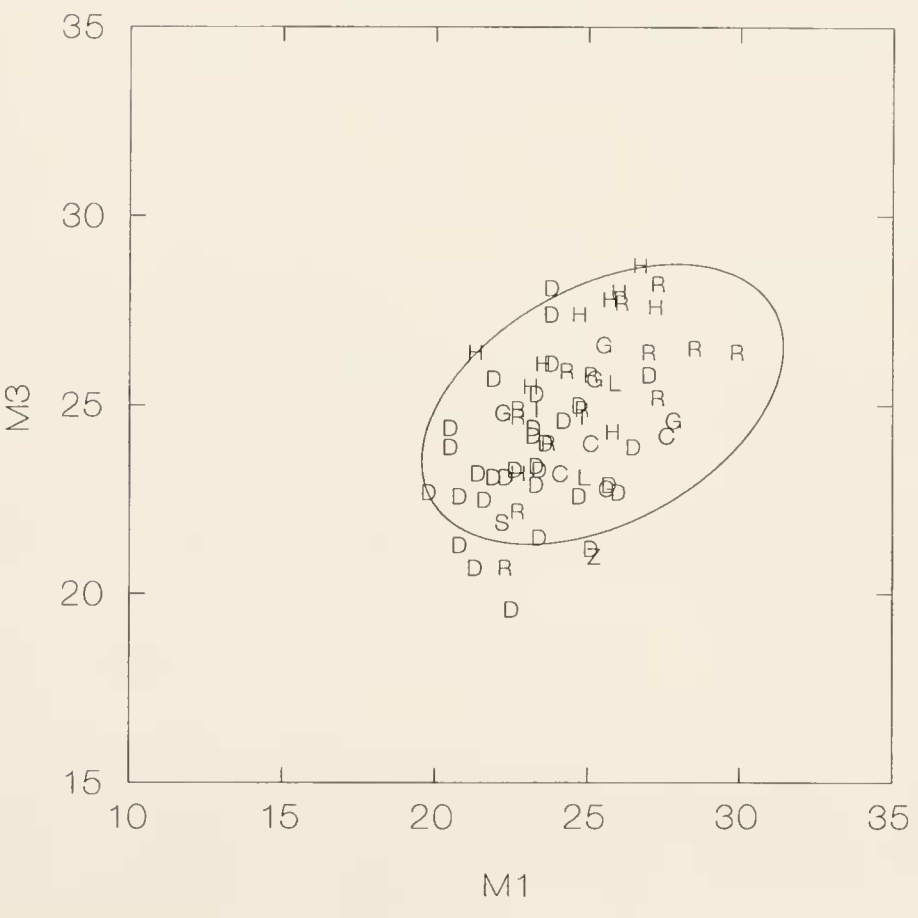
MAXILLARY P4
M3
M1
35
30
25
20
15
10
15
20
25
30
35

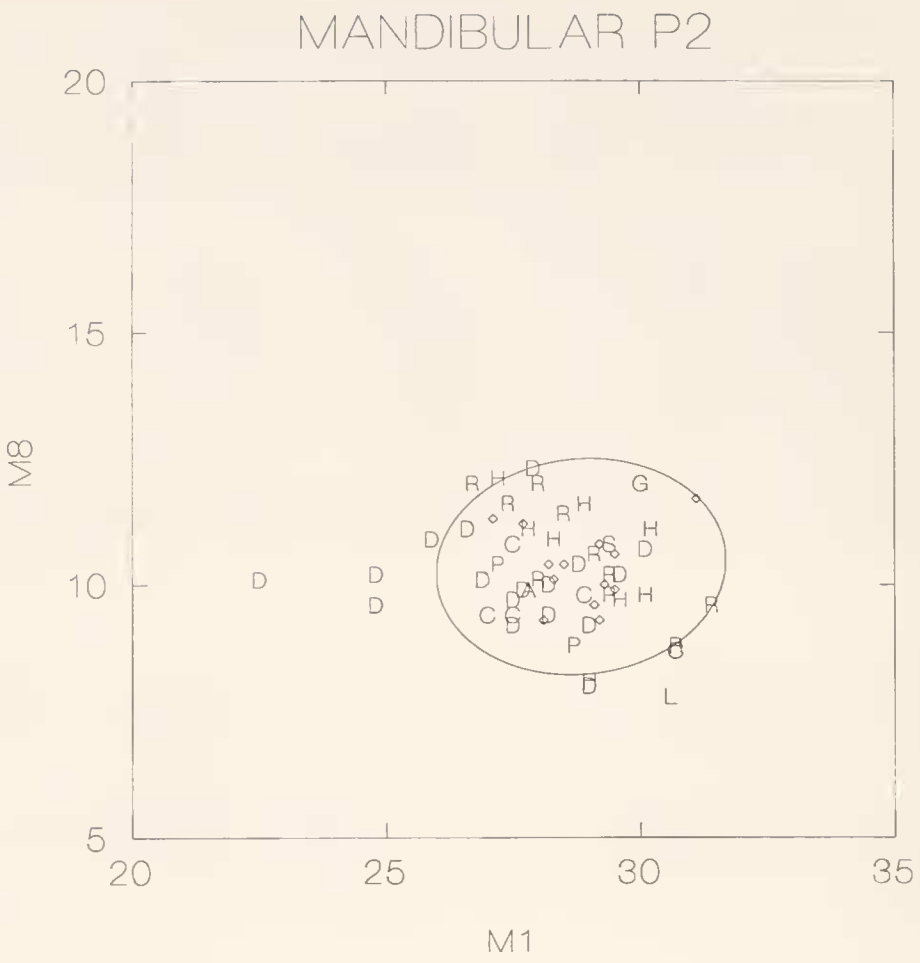
MANDIBULAR P2
M8
M1
20
15
10
5
20
25
30
35

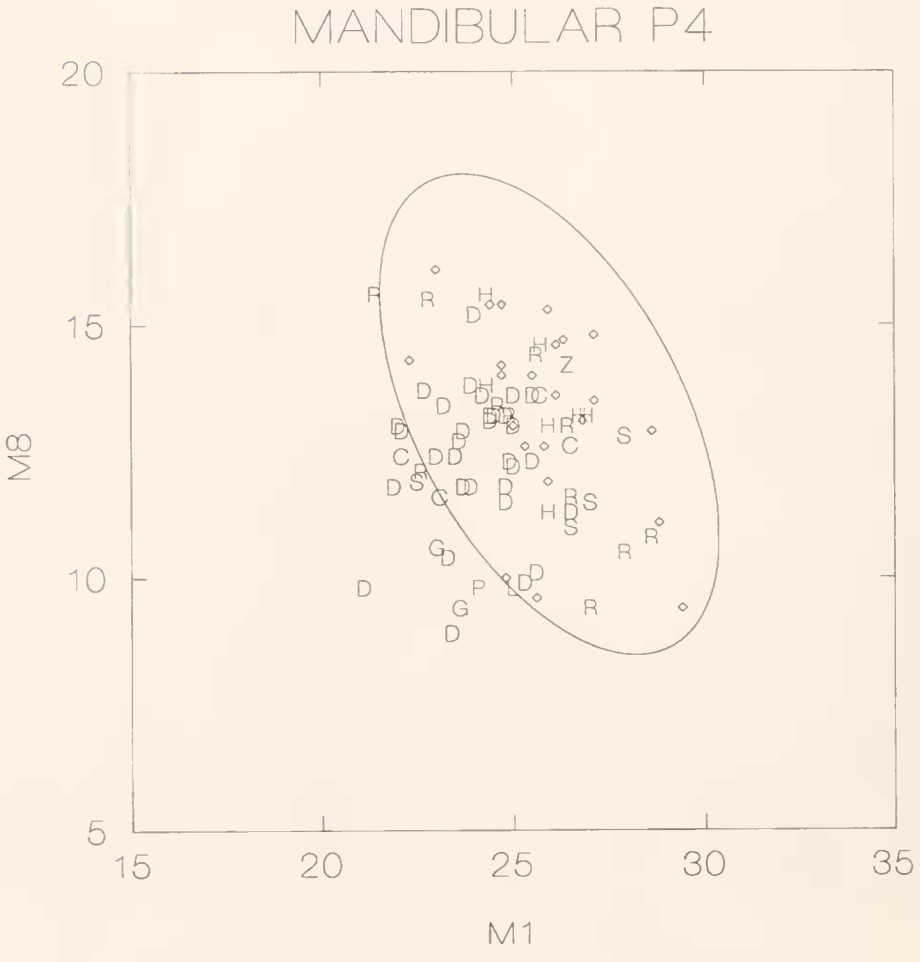
MANDIBULAR P4
M8
M1
20
15
10
5
15
20
25
30
35

maximum length (M1) versus distal articular width (M11), mid-shaft depth (M4) versus mid-shaft width (M3) and proximal articular width (M5) versus proximal articular depth (M6).

There is one Sümeg specimen, the Holotype of "*Hipparion brachypus sumegense*" (MAFIV13242), that is complete enough to preserve the maximum length (M1) dimension (Figure 4a). This individual is well below the Höwenegg 95% confidence ellipse being very short in length. It compares most closely with a short limbed form from MN9 age horizons of Sinap (T). Figure 4b includes several Sümeg specimens for the midshaft (M4 X M3) dimensions. The Holotype of "*Hipparion brachypus sumegense*" is situated just outside the lower edge of the Höwenegg ellipse; indeed, there are two smaller specimens than this which plot further below the ellipse. Yet, there are four Sümeg specimens which plot within the ellipse. The only other specimens found below the ellipse are a specimen from Gols (L) and Sinap (T). Figure 4c plots the proximal articular dimensions (M6 X M5). Once again the Holotype of "*Hipparion brachypus sumegense*" plots on the lower left edge of the Höwenegg 95% confidence ellipse. In this plot there are several specimens plotting to the left of the ellipse, having narrower proximal articular width dimensions (M5), while there is one Sümeg individual that is much smaller than the rest of the sample. This individual we refer below to Hipsm.

3.4.2 Ratio Diagrams for MCIII

We plot two log10 ratio diagrams using the Höwenegg sample mean as our standard. Figure 5a includes an early Vallesian MCIII from Sinap, Turkey believed to be very similar to its North American *Cormohipparion* ancestor (AS93/604A), another derived form from slightly younger early Vallesian levels of Sinap (MNHNTRQ1129), the single complete MCIII known from Dorn Dürkheim (DD4435), a short limbed form from Pannonian D-E horizons of Inzersdorf (Vienna Basin) (NHMW4220c) and the Holotype of "*Hipparion brachypus sumegense*" (MAFIV13242). Interestingly, the Sinap primitive *Cormohipparion* and Dorn Dürkheim specimen are very similar in their morphology suggesting that the latter retains the primitive condition for Central European hipparions, but is more slenderly built than the Höwenegg hipparion. The three shorter MCIII's differ in their length, but also in their ratios: the Sümeg specimen and Sinap specimen are both shorter than the Vienna Basin specimen, but differ from each other in their M3 versus M4 proportions. The Sinap specimen has relatively narrower M3 than M4, while the antithesis is the case in the Sümeg specimen. The Inzersdorf specimen (NHMW4220c) has greater length than these two specimens, but smaller proximal articular width (M5), greater proximal articular depth (M6), and greater distal width (M10, M11) dimensions. This plot suggests that these three "short-limbed" forms are actually different species. While the Vienna Basin individual, NHMW4220C may be ancestral to "*H. brachypus sumegense*", MAFIV13242, the Sinap specimen likely evolved independently of these two Central European forms.

Figure 5b plots the same Dorn Dürkheim and Sümeg (DD4435, MAFIV13242) specimens along with a sample from Csákvár. None of the Csákvár sample is as short as the Sümeg form, and some specimens are substantially longer than the Höwenegg and Dorn Dürkheim samples.

3.4.3 Principal Components Analysis (PCA's) for MCIII

The PCA of MCIII resulted in a first principal component that explained 96% of the total sample variance (Table 4a). Principal component one loaded very heavily with the GEOMEAN

Figure 3: a. Mandibular P2, M8 (occlusal width across metaconid/protoconid) versus M1 (occlusal length); b. Mandibular P4, M8 versus M1.

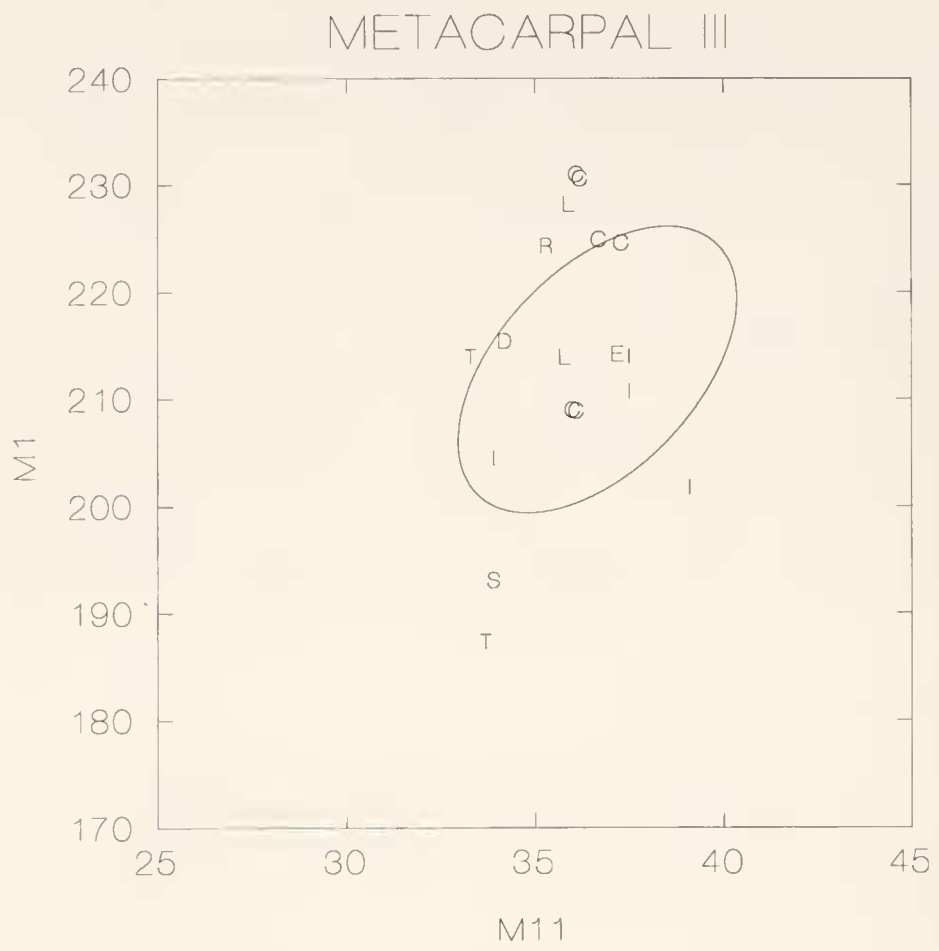
METACARPAL III
240
230
220
210
200
190
180
170
M1
25
30
35
40
45
M11

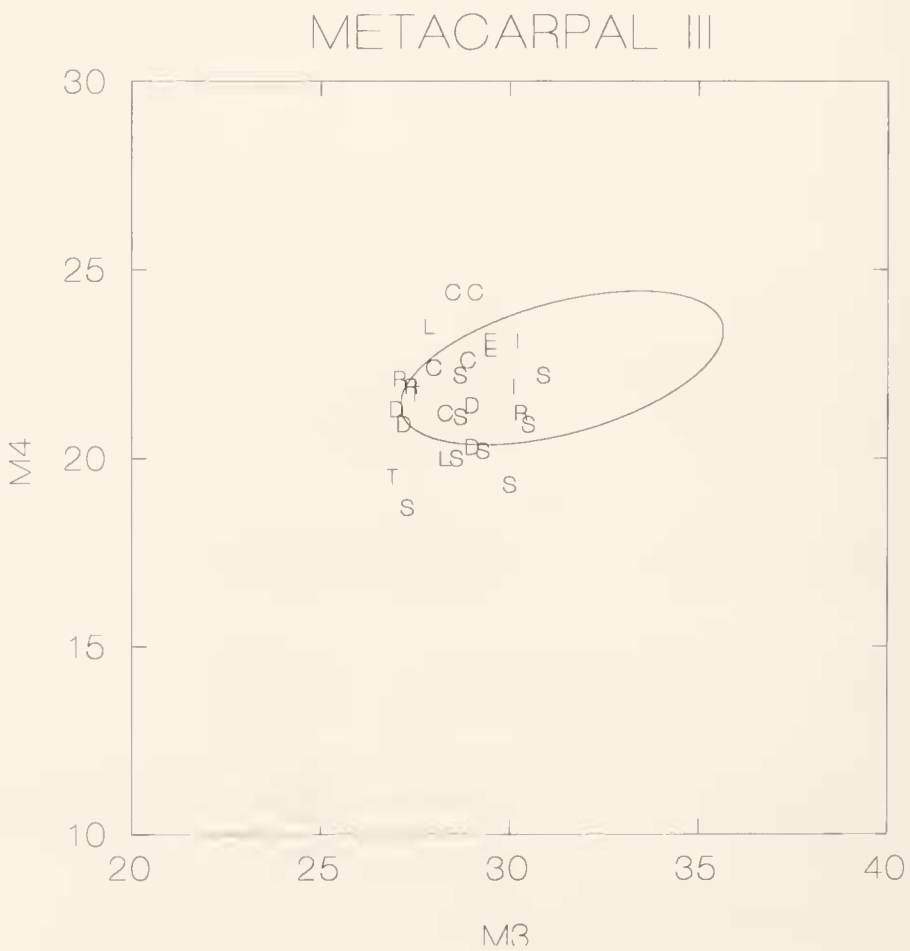
METACARPAL III
30
25
20
15
10
M4
20
25
30
35
40
M3

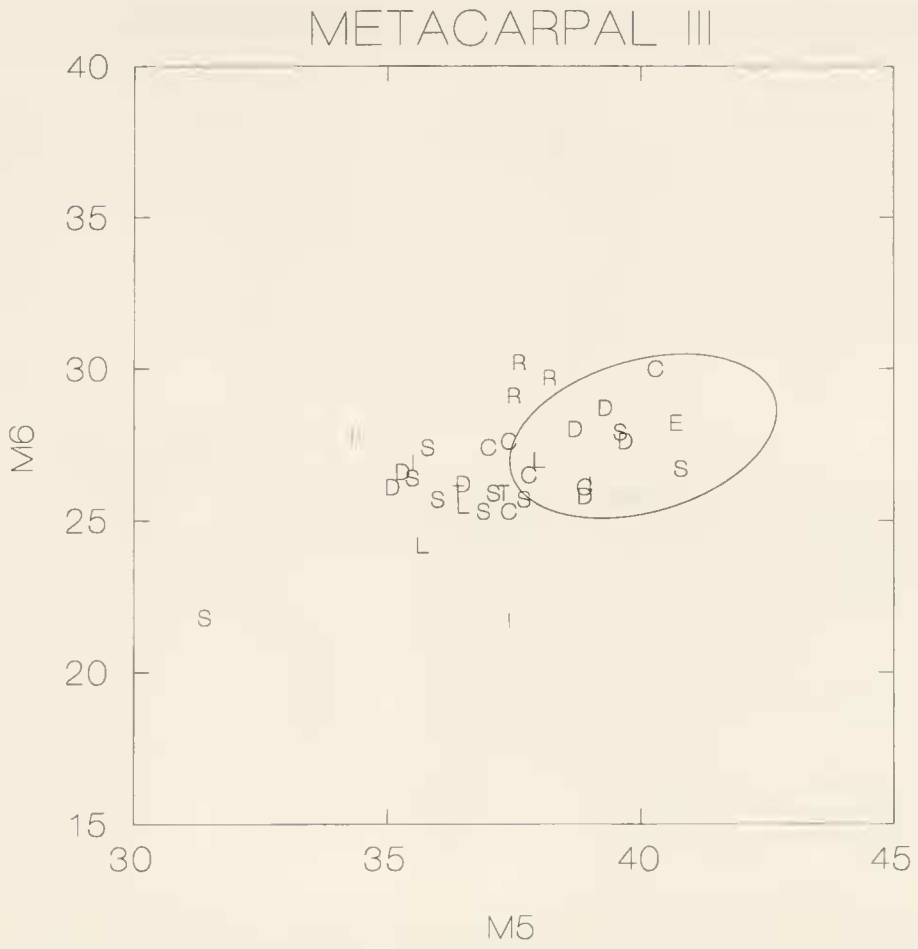

Figure 4: a. Metacarpal III–M1 (maximum length) versus M11 (distal articular width) (type specimen of *Hippotherium sumegense* is indicated by S below the ellipse); b. M4 (mid-shaft width) versus M3 (mid-shaft depth; Type specimen indicated by S just to the right of D [Dorn-Dürkheim specimen], both just at lower border of the ellipse); c. M6 (proximal articular depth) versus M5 (proximal articular width; Type specimen on the lower left border of the ellipse between two C specimens).

corrected value of M2 and had a strongly positive eigenvector with M2 (Table 4b). Thus, principal component one appears to express relative length. Principal component two may also be of interest because of its strongly positive eigenvector with GEOMEAN corrected M3 accompanied by a positive eigenvector for M10 and negative eigenvectors for M4, M5, and M12 (Table 4b). Thus, positive scores on principal component two describe the morphologically interesting pattern of distal mediolateral expansion.

These morphological trends can be interpreted biomechanically, and in turn be linked to locomotor adaptations and habitat preference. Several workers (Eisenmann, 1995; Gromova, 1952; Bernor et al., in prep.) have noted a functional explanation for differences in relative mediolateral or craniocaudal expansion of the metapodials. According to this explanation, metapodial III's that are craniocaudally expanded are adapted to resist greater loads in the sagittal plane such as those that might be generated by cursorial locomotion. One prediction of this model is that hipparionines living in open environments and engaging in cursorial locomotion would have craniocaudally expanded canon bones while forest dwelling species would have mediolaterally expanded canon bones. Thus, we predict that more open country hipparionines are likely to have more negative values for principal component two while closed habitat dwellers are likely to have more positive values for principal component two. Similarly,

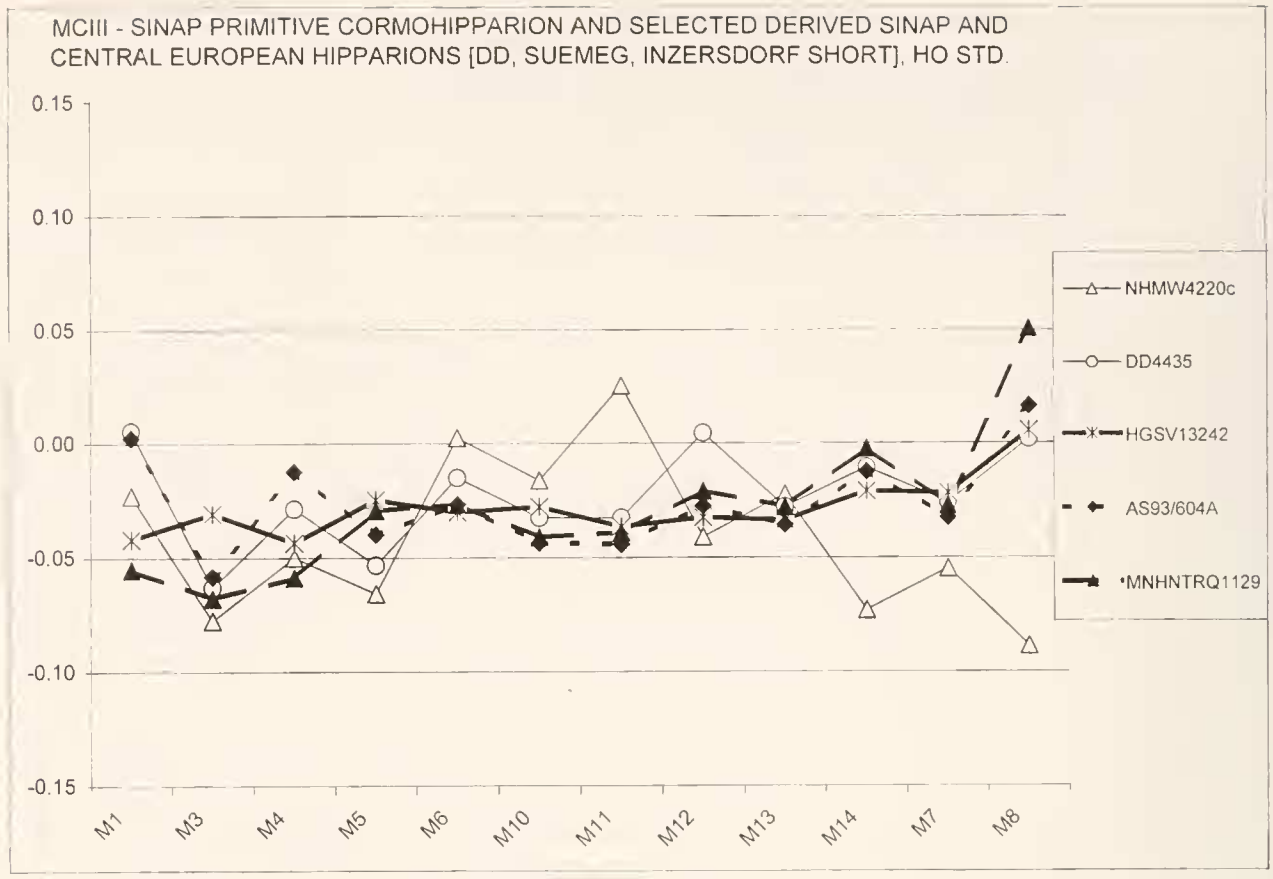

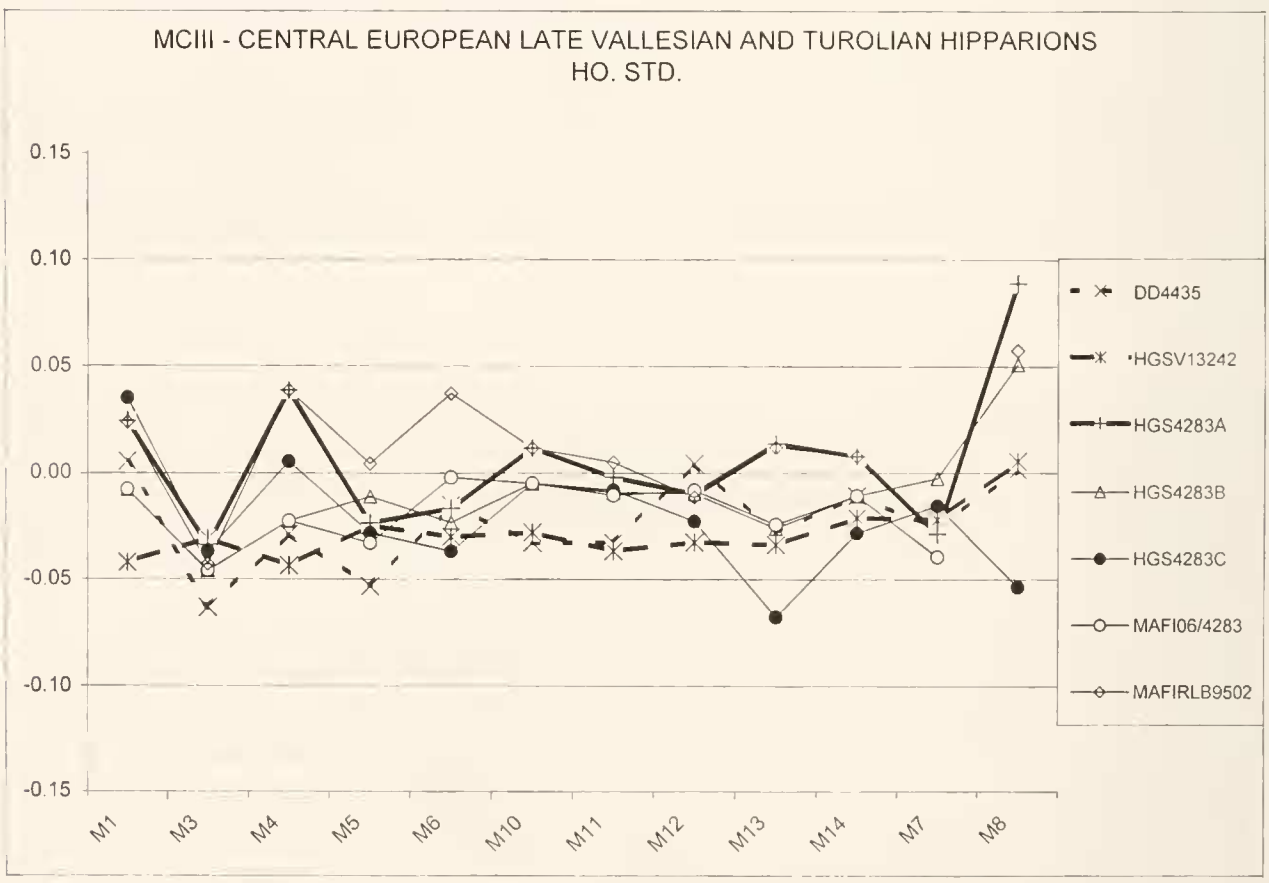

Figure 5: Log 10 Simpson's Ratio Diagrams of Metacarpal III – a. Sinap primitive *Cormohipparion* and selected derived Sinap and Central European hipparions (DD [Dorn Dürkheim], Sümeg, Inzersdorf [short MCIII form], Höwenegg standard; b. Central European late Vallesian and Turolian hipparions, Höwenegg standard.

Table 4: a. Eigenvalues for Principal Components Analysis of Metacarpal III; b Eigenvectors for Principal Components Analysis of Metacarpal III

Principal Component	Eigenvalue	% Variance Explained
One	0.1206	96.1%
Two	0.0022	1.8%
Three	0.0013	1.0%
Four	0.0007	0.6%
Five	0.0007	0.5%
Six	0	0.0%

Variable	Eigenvector					
	Principal Component One	Principal Component Two	Principal Component Three	Principal Component Four	Principal Component Five	Principal Component Six
M2/GEOMEAN	0.9945	0.0513	0.0385	0.022	0.0587	0.0539
M3/GEOMEAN	-0.0688	0.7997	0.1942	0.3524	-0.1672	0.4073
M4/GEOMEAN	0.0081	-0.0596	-0.0239	-0.7132	-0.3548	0.6011
M5/GEOMEAN	-0.0318	-0.4849	0.7415	0.2945	0.0397	0.3546
M10/GEOMEAN	-0.0701	0.0838	-0.1189	-0.1397	0.9033	0.372
M12/GEOMEAN	0.0151	-0.335	-0.6295	0.5103	-0.1585	0.4536

the observation that cursorial forms generally have elongate limbs suggests that hipparionines with high scores for principal component one are likely to have low scores for principal component two. MCIII's with positive scores for principal component one and negative scores for principal component two will be long and relatively slender suggesting adaptation for cursorial locomotion.

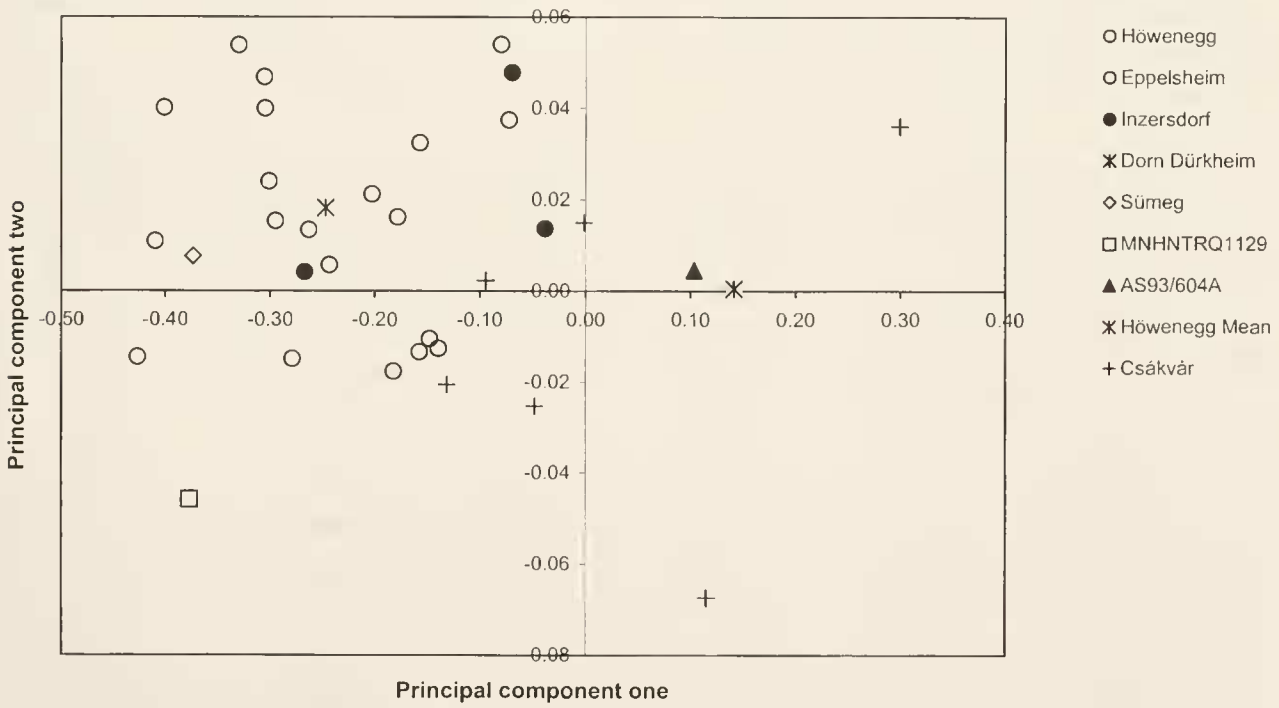

Figure 6: Principal Components Plot of Components 1 and 2 for MCIII. The single Sümeg specimen, MAFIV13242, is plotted relative to specimens from Höwenegg, Inzersdorf, Dorn Dürkheim, Eppelsheim, Sinap, and Csákvár.

The Höwenegg hipparionine sample has previously been interpreted as belonging to a single, forest dwelling species capable of leaping and springing (Bernor et al., 1997). This suggestion is supported by our PCA results where the Höwenegg MCIII sample exhibits a relatively short and broad morphology (see Figure 6). The cluster of points here in the second quadrant confirms our suspicion that the Höwenegg hipparion probably was adapted for less sustained, straight-forward cursorial behavior appropriate for a forested environment. A sample of hipparionine metapodials from another site that encompasses more variation than exhibited for the Höwenegg specimens in all likelihood represents more than one species. Similarly, metapodials with principal component scores similar to those from Höwenegg were possibly similarly forest-adapted species, while cursorial species would be predicted to plot opposite the Höwenegg sample in the fourth quadrant.

A single MCIII specimen from Sümeg, MAFIV13242, the Holotype of *Hippotherium sumegense*, plots within the polygon for the Höwenegg sample in Figure 6. However, the principal component scores for both principal components one and two are at the extreme edge of the Höwenegg sample. For principal component one, MAFIV 13242 is below the 95% confidence limit for the Höwenegg sample. For principal component two, MAFIV13242 is just within the 95% confidence limits for the Höwenegg sample. Thus, MAFIV13242 would appear to be relatively short compared to the Höwenegg sample as well as possibly different in terms of shaft morphology. MAFIV13242 also appears to be distinct when compared to other short-limbed forms. For example, the specimen MNHNTRQ1129 from Sinap, Turkey represents a derived, short metapodial form. MNHNTRQ1129 clearly plots differently with regard to principal component two than MAFIV13242. Indeed, the negative score of MNHNTRQ1129 for principal component two confirms the contrasting morphologies of these two specimens suggested by the ratio diagram shown in Figure 5a. MNHNTRQ1129 from Sinap would appear relatively more slender distally and at midshaft than MAFIV13242 from Sümeg where M3 is greatly expanded compared to M4.

The other short-limbed form, NHMW4220c from Inzersdorf (Vienna Basin, MN9; Bernor et al., 1988; Figure 5a here) could not be included in our PCA analysis because of a missing M3 measurement. However, MAFIV13242 contrasts with the three complete specimens from Inzersdorf that were available for analysis. While these specimens are somewhat heterogeneous with respect to their PCA scores, none of them plot near MAFIV13242 (Figure 6). Thus, our PCA analysis confirms the unique position of MAFIV13242.

The contrasts previously noted between MAFIV13242, AS93/604A from Sinap, the single complete MCIII from Dorn Dürkheim (DD4435), and specimens from Csákvár are confirmed by our PCA analysis. These specimens are uniformly relatively longer than MAFIV13242. Several of the Csákvár specimens have negative scores on principal component two indicating greater relative slenderness. In summary, principal components analysis confirms that MAFIV13242 is unique from the standpoint of MCIII morphology.

3.4.4 Scaling of MCIII

One potential cause of the apparent distinctiveness of MAFIV13242 could be body size. Thus, the question must be asked: "Could the morphological pattern apparent for this specimen simply be a function of body size?" The body mass estimate determined here for MAFIV13242 was 199 kg which was slightly outside the range of body mass estimates for the Höwenegg sample of 202 kg to 270 kg. This fact complicates comparisons between the Höwenegg sample and MAFIV13242 because predicted values for dimensions of MAFIV13242 based on the Höwenegg sample require extrapolating outside the size range for the Höwenegg sample. Thus, residuals were calculated for MAFIV13242 based on regressions for the entire available sample (n=90) (Table 5a).

Table 5b reports the standardized residuals from the regressions of M6 and the six variables included in the PCA against estimated body mass for MAFIV13242 as well as the regression statistics for each of these regressions. Negative residuals are evident for the craniocaudal dimensions M4 (mid-shaft craniocaudal length), M6 (proximal articular surface craniocaudal length), and M12 (craniocaudal length of distal mid-sagittal keel), as well as for the length dimension M2. Positive residuals are the case for the mediolateral dimensions M3 (mid-shaft width) and M5 (proximal articular surface width). The mediolateral dimension M10 has a negative residual but this value is small indicating little deviation from the dimension expected based on estimated body mass. Thus, what these regressions confirm is that MAFIV13242 departs from the proportions expected based on its estimated body mass in several respects. The most diagnostic dimensions for MAFIV13242 are greatly reduced length (M2), a greatly reduced craniocaudal dimension at midshaft (M4) and an expanded mediolateral dimension at midshaft (M3). The regressions for these three dimensions are shown in Figure 7a-c in conjunction with the Höwenegg sample.

The residuals for MAFIV13242 are in many respects similar to those of the short Sinap

Table 5: a. Standardized residuals of selected specimens for key variables regressed versus estimated body mass; b. Regression statistics for key variables versus estimated body mass.

Dependent Variable	**r-squared**	**Standardized Residuals**				
		Howenegg mean	MAFIV13242	MNHNTRQ1129	DD4435	AS93/604A
M2	0.40	-0.17	-1.81	-2.17	0.86	0.55
M3	0.89	0.73	1.23	0.21	-0.02	0.09
M4	0.78	-0.26	-1.04	-1.18	-0.04	0.66
M5	0.84	0.26	0.51	0.98	-0.70	-0.09
M6	0.76	-0.41	-0.52	0.20	0.42	-0.19
M10	0.95	-0.22	0.36	0.58	0.58	-0.54
M12	0.69	-0.44	-0.54	0.45	1.30	-0.17

Dependent Variable	*Intercept/Slope*	*Coefficients*	*Standard Error*	*t*	*P*
M2	Intercept	1.986	0.042	47.313	2.2843E-64
M2	Slope	0.140	0.018	7.673	2.1425E-11
M3	Intercept	0.375	0.041	9.164	1.8887E-14
M3	Slope	0.465	0.018	26.100	3.3513E-43
M4	Intercept	0.553	0.043	12.766	9.8639E-22
M4	Slope	0.337	0.019	17.817	6.1404E-31
M5	Intercept	0.744	0.039	19.160	3.7455E-33
M5	Slope	0.358	0.017	21.165	2.7682E-36
M6	Intercept	0.648	0.046	13.963	4.8688E-24
M6	Slope	0.336	0.020	16.624	6.8741E-29
M10	Intercept	0.587	0.025	23.552	9.2066E-40
M10	Slope	0.424	0.011	39.021	2.4518E-57
M12	Intercept	0.749	0.048	15.539	5.8628E-27
M12	Slope	0.294	0.021	14.018	3.842E-24

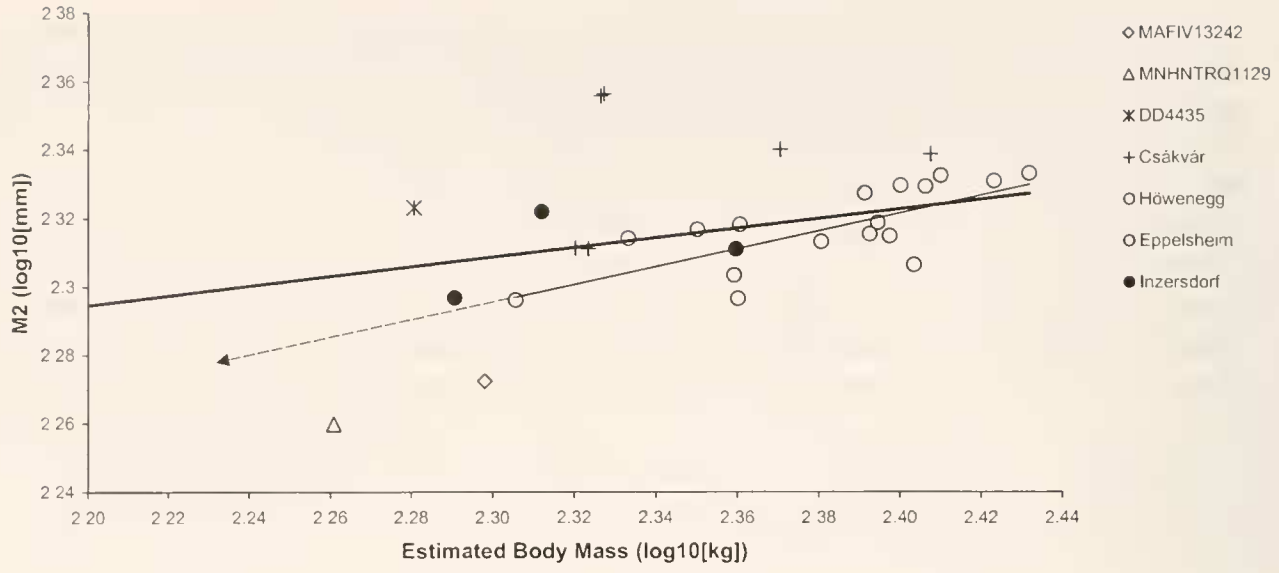
M2 (log10[mm])
Estimated Body Mass (log10[kg])
MAFIV13242
MNHNTRQ1129
DD4435
Csákvár
Höwenegg
Eppelsheim
Inzersdorf

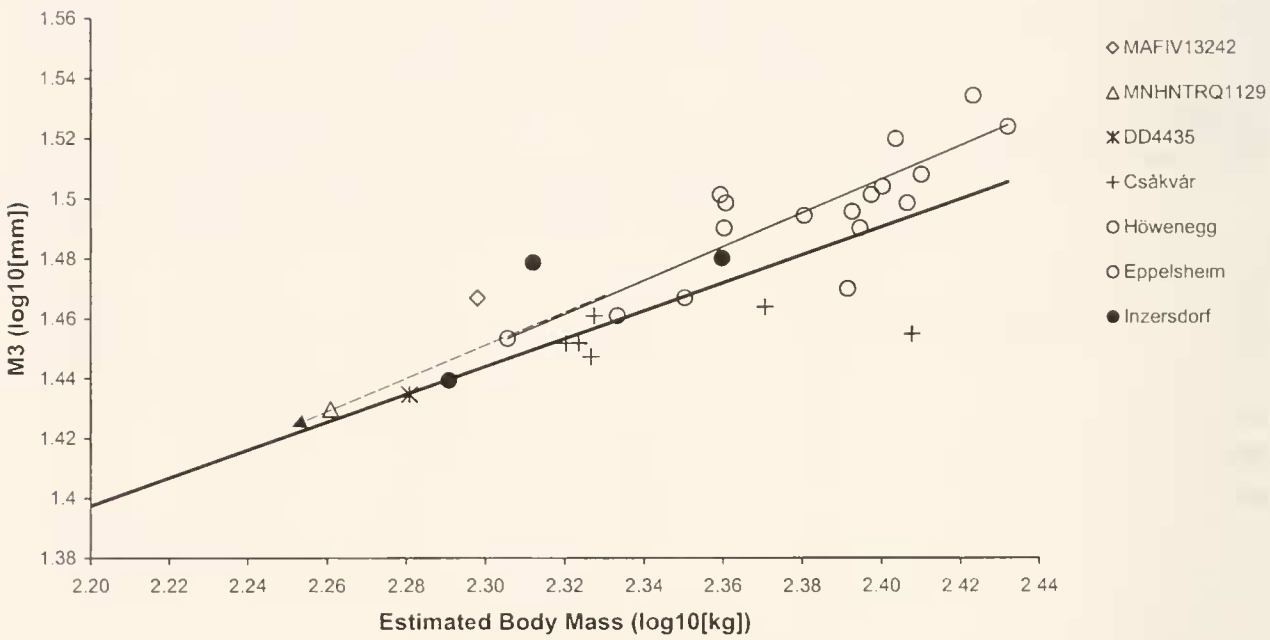
M3 (log10[mm])
Estimated Body Mass (log10[kg])
MAFIV13242
MNHNTRQ1129
DD4435
Csákvár
Höwenegg
Eppelsheim
Inzersdorf

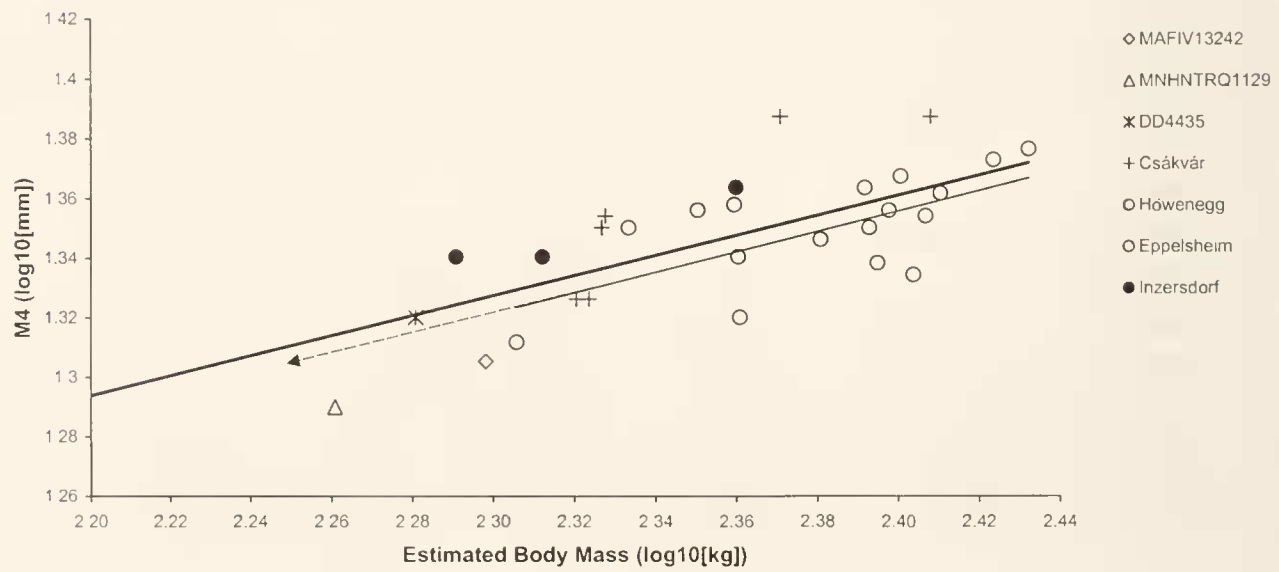
M4 (log10[mm])
Estimated Body Mass (log10[kg])
MAFIV13242
MNHNTRQ1129
DD4435
Csákvár
Höwenegg
Eppelsheim
Inzersdorf

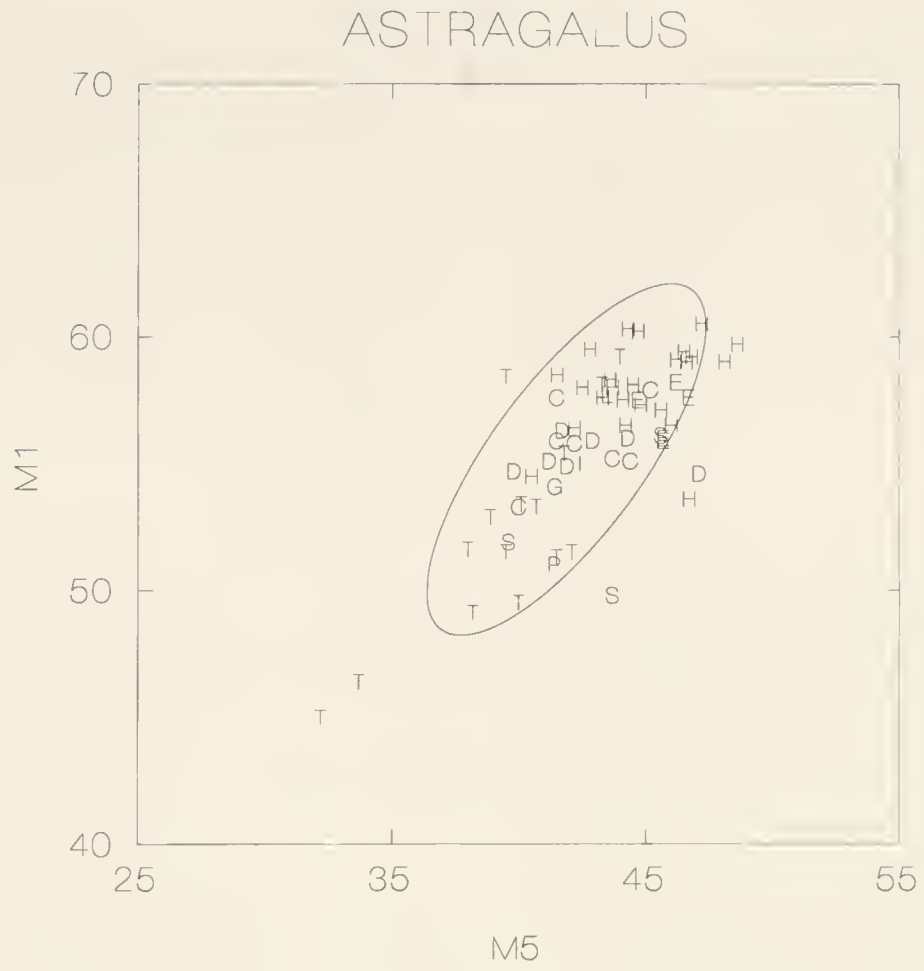

Figure 8: Astragalus - M1 (maximum length) versus M5 (distal articular width).

specimen, MHNTRQ1129, with the exceptions of M3, M6, and M12. Measurement 3 has a much lower residual value for MNHNTRQ1129, and positive as opposed to negative residual values for M6 and M12 (see Table 5). Further study of these scaling relationships is certainly desirable, however, what can be determined from this preliminary investigation is that the evident shortening and flattening described for MAFIV13242 can not simply be attributed to scaling but rather is likely to have some adaptive and/or phylogenetic significance.

3.4.5 Bivariate Plots for the Posterior Limb

Figure 8 calculates maximum length (M1) versus distal articular breadth (M5) for astragali. There are two Sümeg specimens that plot within the Höwenegg ellipse, one in the lower portion and the other on the right edge of the ellipse. A third specimen plots outside the ellipse, with a low M1 value and relatively high M5 value.

Figure 7: a: – Least squares regression of M2 versus estimated body mass. The thick line represents the regression for the entire sample and the thin line represents the regression for the Höwenegg sample only. The dashed extension of the Höwenegg line represents a linear extrapolation outside the size range of the Höwenegg sample.; b. Least squares regression of M3 versus estimated body mass. The thick line represents the regression for the entire sample and the thin line represents the regression for the Höwenegg sample only. The dashed extension of the Höwenegg line represents a linear extrapolation outside the size range of the Höwenegg sample; c: Least squares regression of M4 versus estimated body mass. The thick line represents the regression for the entire sample and the thin line represents the regression for the Höwenegg sample only. The dashed extension of the Höwenegg line represents a linear extrapolation outside the size range of the Höwenegg sample.

4 Systematics

4.1 Taxonomy

Order Perissodactyla Owen 1848

Suborder Hippomorpha Wood 1937

Superfamily Equoidea Hay 1902

Family Equidae Gray 1821

Subfamily Equinae Steinmann & Döderlein 1890

Hippotherium sumegense (Kretzoi, 1984)

Type: MAFIV13242, a left metacarpal III

Type Locality: Sümeg

Referred Specimens: listed in Tables 1, 2 and 3 here

Age: Late Miocene, late Vallesian age (MN 10), ca. 9.5-9.0 Ma. (re: Rögl & Daxner-Höck, 1996; Steininger et al., 1996).

Geographic Range: Pannonian Basin, Central Paratethys

Diagnosis [with derived characters in bold]:

A smaller member of the Central European *Hippotherium primigenium* – lineage **with short MCIII that has a relatively broad and flat midshaft dimension**; cheek teeth moderately curved; maximum crown height probably circa 50 mm; **posterior wall of postfossette always separate from distal enamel wall of the tooth**; pli caballins variably double or **single**; hypoglyph deep; **protocones usually oval** and isolated from protoloph; **protoconal spur very rare and small when present; premolar and molar protocone placed lingual to hypocone; premolar metaconid elongate and sub-square shaped while metastylid has an irregular "goblette" shape; no observed incidence of ectoflexid extending between metaconid and metastylid**; pli caballinid single or rudimentary or absent; **protostylid is a reduced pointed projection that often courses obliquely to the anterior surface of the tooth rising only slightly on the anterior surface of the tooth**; ectostylids are absent in adult cheek teeth; **linguaflexid is very broad and shallow often being interrupted by a large metastylid spur**; preflexids and postflexids vary in their degree of complexity; postflexid does not bend sharply anteriorly; **protoconid enamel band exhibits limited flattening medially.**

Remarks:

Kretzoi (1984) originally referred the Holotype MCIII MAFIV13242 to *Hipparion brachypus sumegense*. The nomen *Hipparion brachypus* was first applied to an assemblage of relatively short and broad MCIII's from Pikermi by Hensel (1862), but no type specimen was designated and the figured assemblage was lost (Koufos, 1987). Koufos (1987) revised the material from Pikermi referring a large-sized hipparion with short robust metapodials to *Hipparion brachypus*. There is a cast of a forefoot, figured by Abel (1927) that Heissig believes might be a suitable candidate for the Lectotype of *H. brachypus*. Bernor et al. (1996) suggested that this species may be referable to the genus *Hippotherium*. Referring to Table 33 in Koufos' (1987) study of the Pikermi hipparions, we find that the mean maximum length (M1) of *H. brachypus* is 211.3, versus 193.1 in the Holotype *Hippotherium sumegense*; likewise M3 in *H. brachypus* is

30.7, versus 29.3 in *H. sumegenense* and distal articular width is 37.9 in the Pikermi form and 33.9 in the Sümeg species. The Holotype *H. sumegense* is clearly different from the Pikermi form and best recognized as a distinct species.

The most distinguishing feature of the lower cheek teeth referred to *Hippotherium sumegense* is the irregular, large goblet-shaped metastylids of the premolars. There is no evidence of this morphology in the molars. Irregular, small star-shaped metastylids occur in very early stage-of-wear of Central European MN9 *Hippotherium primigenium*. These star-shaped metastylids persist later in adult wear and often become larger, goblet-shaped morphs in later Vallesian Pannonian Basin assemblages such as Prottes, Götzendorf and Sümeg, and that is the reason why we think it distinctly possible that these three localities may all be MN10 correlative (but see Rögl et al., 1993 for alternative arguments).

"*Hipparion*" sp. small (Hipsm)

There is a second, rarer small taxon in the Sümeg sample represented by a fragmentary MCIII (MAFIV13244G) and 4 cheek teeth (specimen # 5a, 5b, 6, 7) (Tables 1–3). The MCIII was labeled "*Hipparion matthewi*" by Kretzoi, and indeed it is possible that this specimen could be related to the *Cremohipparion macedonicum – Cremohipparion matthewi – Cremohipparion nikosi – Cremohipparion periafricanum* lineage recently discussed by Bernor et al. (1996). This lineage first occurs in MN10 of Greece (Koufos, 1987; Bernor et al., 1996), so it is not out of place chronologically in its occurrence at Sümeg. Nevertheless, the material is simply too limited to determine this relationship exactly.

5 Paleoecology

5.1 MCIII Ecomorphology

Based on the MCIII morphology of MAFIV13242 already described, we infer that *Hippotherium sumegense* most likely preferred closed habitat surroundings. The relatively short length and mediolaterally expanded shaft exhibited by MAFIV13242 suggests a reduced emphasis on sustained cursorial behavior and is most consistent with more closed surroundings. A mediolaterally expanded MCIII shaft could resist loads in various directions such as those that might be generated in a habitat with twisting paths over soft substrates. Such environments are most likely to be found in closed woodland or forested areas where downed timber, other obstacles, and moist ground are more likely. The relatively short MCIII suggests a shortened limb and reduced leverage facultative for slower, less sustained running and sure-footedness. Thus, a predator avoidance strategy relying on crypsis is more likely than one of sustained high speed flight in open areas.

5.2 Macroscopic Occlusal Wear Features

The Sümeg upper cheek teeth have a strongly developed bucco-lingual groove which courses across the entire occlusal surface from the mesostyle to the center of the protocone. The groove is deepest at the mesostyle. Mesial and distal to this groove are two high and sharp crests, which course across the entire occlusal surface of the cheek tooth in parallel to the central groove structure, dividing the pre- and postfossettes into two with steep slopes flanking a central ridge. On the buccal side the crests are formed by angular projections of the ectoloph immediately

A-b-1
A-b-2
B-b-1
B-b-2
C-b-1
C-b-2
D-b-1
D-b-2
2 mm
A-b
B-b
C-b
D-b
A
B
C
D
10mm

labial to the pre- and postfossettes. These projections show different degrees of rounding, and in rare cases seem to have sharp edged tips. Grooving depth and ectoloph sharpness varies amongst Old World Neogene hipparion species and is believed to be related to diet so that deep grooving is indicative of a higher browse component while occlusal flatness, as is apparent in modern zebra, is indicative of a diet dedicated to grazing (BERNOR and ARMOUR-CHELU, in press). The recent work of FORTELIUS and SOLOUNIAS (in press) has developed a far more sophisticated statistical means of evaluating diet based on occlusal wear features, and we await publication of their work to employ their methodology on equids. Our evaluation here is merely qualitative and meant to exemplify the differences between some Central European hipparions with marked grooving of the occlusal surface and a modern grass-eating zebra. We use characteristic maxillary M1 and M2 specimens from Sümeg (specimens #4 and #7), from Rudabánya (MAFIV12125), from Eppelsheim (HLMDDIN 2716), and a recent specimen of *Equus burchelli* (SENK19210; Figure 9, here).

Description of occlusal grooving:

Sümeg specimen #4 (left txM2; Hsum; Figure 9A, 9Ab, 9Ab 1–2) has a deep bucco-lingual groove. This courses across the midline of the tooth (from mesostyle to the middle of the protocone) and rises mesially and distally to form two ridges that dissect the pre- and postfossette into two equal halves (re: Figure 9). The ectoloph is slightly rounded apically lateral to the paracone, while absent lateral to the metacone. The mesial and distal flanks are oriented at an angle of nearly 95° (Figure 9Ab).

Eppelsheim specimen HLMDDIN 2716 (right txM2; Figure 9B, 9Bb, 9Bb1–2) also exhibits strongly developed bucco–lingual grooving (Figure 9Bb). The groove morphology is U-shaped with less straight edges formed by the ectoloph (Figure 9Bb1, 9Bb2). The grooving pattern is slightly less deep and the rounding of the mesial and distal ectoloph is slightly more pronounced than in the Sümeg specimen.

Rudabánya specimen MAFIV12125 (left txM2; Figure 9C, 9Cb, 9Cb1–2) is similar to the Sümeg and Eppelsheim specimens with bucco-lingual grooving being strongly developed. The groove morphology is U-shaped with flanks of the mesial and distal ectoloph being comparable in straightness to the Sümeg and the Eppelsheim specimens (Figure 9Cb1, 9Cb2). The rounding of the mesial and distal ectoloph is less pronounced than in the Sümeg and the Eppelsheim specimens. The cusp apex of the distal ectoloph enamel band at the buccal aspect is sharply edged and does not show significant rounding.

In *Equus burchelli boehmi* SENK19210 (8–10 year old male; left txM2; Figure 9D, 9Db, 9Db1-2) bucco-lingual grooving is poorly developed. The groove morphology is a broad, shallow U-shaped morphology and much less deeply incised in the occlusal surface than in the hipparion specimens in this comparison. The rounding of the paracone – metacone cusp apices on the buccal aspect is similar to the Sümeg and the Eppelsheim specimen, however the relief of the cusp apices is far less pronounced than in the hipparions.

Figure 9: Macroscopic occlusal features including grooving and ectoloph apical morphology. A, Ab, Ab1-2: Sümeg specimen #4 (left txM2); B, Bb, Bb1-2: Eppelsheim specimen HLMDDIN 2716 (right txM2, mirrored in figures); C, Cb, Cb1-2: Rudabánya MAFIV12125 (left txM2); D, Db, Db1-2; SENK19210 (*Equus burchelli boehmi*, 8-10 year old male; left txM2). A; B; C; D occlusal aspect (left = mesial). Bucco-lingually oriented crest structures, which distally and mesially bracket a central groove are highlighted by dotted lines. Ab, Bb, Cb, Db buccal aspect of apical crown portions. Ab1/2; Bb1/2; Cb1/2; Db1/2: apical portion of ectoloph apices of paracone (left) and metacone (right); see frames.

A
B
C
D
30μm

We realize apparent differences between the hipparion molars in this comparison and the recent zebra specimen. These differences are in the relative depth of the central groove structure and in the relief of the adjoining crests. In *Equus* the groove appears shallow, showing a broad U-shaped bottom morphology with gently curved flanks. In the hipparions this groove is steeper, deeper and more distinct. The bucco-lingual crests have highly elevated and distinct crest apices in the hipparions, in the *Equus* specimen the crests appear to be rounded and only a little distinct. In the hipparions, crest tips at the ectoloph are slightly rounded with the exception of the Rudabánya specimen, where the distal ectoloph appears angular and sharp crested buccally.

In this comparison, we find the bucco-lingual groove to be most deeply incised in the Sümeg specimens, and the least distinct in *Equus*. We predict that the macroscopic occlusal wear features will be found to be closely correlative with masticatory action and food quality and quantity. We tentatively conclude that the dietary regimens of the hipparion species we report on here are more similar to each other than to *Equus*.

5.3 Tooth Microwear Comparison

We document tooth microwear patterns in the Sümeg cheek tooth assemblage and compare them to specimens from the Dinotheriensands and from Rudabánya. Specimens available for this study included Sümeg specimens listed in tables 2–3, 21 upper M2 specimens from the Dinotheriensands and left tmP2–tmM3 (MAFIV15795) and txP3-txM2 (MAFIV15749) from Rudabánya. Figured specimens include (Figure 10): Sümeg specimen #4 (txM2); Sümeg specimen #7 (txM1); Eppelsheim specimen HLMDDIN2716 (txM2) and Rudabánya specimen MAFIV15749 (txM1).

Microwear features predominating in all samples studied are scars dichotomised into pits and scratches (striations) by various workers (Rensberger, 1978; Solounias et al., 1988; Teaford & Walker, 1984; Van Valkenburg et al., 1990; Teaford, 1991; Solounias & Hayek, 1993). Comparing the overall appearance of microwear features in the *Hippotherium sumegense* assemblage from Sümeg, both scratches and pits are equally present on the occlusal surface (Figure 10a). One specimen assigned to the small hipparion species from Sümeg (#7; Figure 10b) shows a predominance of scratches, but pits still are present. The Sümeg assemblage shows most similarities with specimens of *Hippotherium primigenium* from Eppelsheim (Figure 10c), which also show a pit dominated microwear pattern. In both samples, areas of polished enamel are more or less extended between the scars. The Rudabánya specimens studied show more scratching and less pitting than the Sümeg and Eppelsheim specimens (Figure 10d), with the exception of Sümeg specimen #7 (Figure 10b), which has most similarities with the Rudabánya material studied. In both the Rudabánya specimen and Sümeg specimen #7 there is only very little unscratched enamel surface exposed.

The frequency and morphology of enamel scars as pits and scratches are believed to be controlled by dietary regimes and functional masticatory parameters (Hayek et al., 1992; Hunter & Fortelius, 1994). In herbivorous mammals, the proportion of pits to scratches is one of the microwear characters regarded important for species segregation by Hayek et al. (1992), and is used for inferring dietary behavior (Solounias & Moelleken, 1992, 1993, 1994).

Figure 10: SEM-micrographs of the occlusal surface of the ectoloph labial to the paracone (x500) showing representative microwear features. Buccal is towards the left. A: Sümeg specimen #4 (txM2); B: Sümeg specimen #7 (txM1); C: Eppelsheim HLMDDIN2716 (txM2); D: Rudabánya MAFIV15749 (txM1).

Solounias & Hayek (1993) report that with some exceptions, recent browsers had fewer scratches and more pits than grazers; the converse is true in grazers. The predominance of scratches in Sümeg specimen #7 and the Rudabánya specimen may thus suggest a higher proportion of grass in the last meal of these specimens. On the other hand, the more pitted overall appearance of Sümeg specimen #4 and the Eppelsheim sample would indicate higher proportions of softer food matter. This is also suggested by the presence of extended polished areas. These polished and featureless areas are considered to be controlled by occlusal enamel-enamel attrition, as demonstrated by Teaford & Walker (1983). We thus expect considerable attrition control in microwear features of the Sümeg specimen #4 (Figure 10a) and in the Eppelsheim specimen HLMDDIN2716 (Figure 10c). We are aware of the fact that this qualitative comparison is provisional, however, it does indeed point to differences in the microwear of Sümeg specimens #4, *H. sumegense*, and #7 *H. sp.* small.

6 Acknowledgements

We wish to thank OTKA (Hungary), the National Geographic Society, L.S.B. Leakey Foundation, Alexander Von Humboldt Stiftung and the US-Hungarian Cooperative Research Program administered by Ms. Francine Berkowicz (Smithsonian Institution) for funding our research on the Rudabánya and other Central European hipparionine horses.

7 Literature cited

Abel, O. (1927): Lebensbilder aus der Tierwelt der Vorzeit. Jena, Verlag von Gustav Fischer. 1–679.

Bachmayer, F. & R.W. Wilson (1970): Small Mammals (Insectivora, Chiroptera, Lagomorpha, Rodentia) from the Kohfidisch Fissures of Burgenland. Austria. – Ann. Naturhist. Mus. **74**: 533–587. Wien.

Bachmayer, F. & W. Wilson (1984): Die Kleinsäuger von Götzendorf, Niederösterreich. – Sitzungsberichte der Österr. Akademie der Wissenschaften, Mathem.-naturw. Kl., Abt. I, **193**(6): 303–319. Wien.

Bernor, R.L. & J. Franzen (1997): The equids (Mammalia, Perissodactyla) from the late Miocene (Early Turolian) of Dorn-Dürkheim 1 (Germany, Rheinhessen). – Courier Forschungsinstitut Senckenberg. **197**: 117–186. Frankfurt.

Bernor, R.L. & M. Armour-Chelu (1996): Later Neogene Hipparions from the Manonga Valley, Tanzania. – In: Harrison, T. (ed.): Neogene Paleontology of the Manonga Valley, Tanzania. Plenum: New York. pp. 219–264.

Bernor, R.L. & M. Armour-Chelu (1999): Towards an Evolutionary History of African Hipparionine Horses – In: Bromage, T. & Schrenk, F. (eds.): African Biogeography, Climate Change and Early Hominid Evolution, Wenner-Gren Foundation Conference, Livingstonia Beach Hotel, Salima, Malawi. Oxford: Oxford.

Bernor, R.L. & D. Lipscomb (1991): The systematic position of "*Plesiohipparion*" *aff. huangheense*, Gülyazi, Turkey. Mitteilungen der Bayerischen Staatssammlung für Paläontologie und historische Geologie. **31**: 107–123. München.

Bernor, R.L. & D. Lipscomb (1995): A consideration of Old World hipparionine horse phylogeny and global abiotic processes. – In: Vrba E. et al. (eds.): *Paleoclimate and Evolution with Emphasis on Human Origins*. Yale University Press: New Haven. pp. 164–177.

Bernor, R.L., G. Koufos, M.O. Woodburne & M. Fortelius (1996): The evolutionary history and biochronology of European and Southwestern Asian late Miocene and Pliocene hipparionine horses. – In: Bernor, R.L., V. Fahlbusch & H.-W. Mittmann (eds.): *The Evolution of Western Eurasian Later Neogene Mammal Faunas*. Columbia University Press: New York. pp. 307–338.

Bernor, R.L., H. Tobien, L.-A. Hayek & H.-W. Mittmann (1997): *Hippotherium primigenium* (Equidae, Mammalia) from the late Miocene of Höwenegg (Hegau, Germany). – Andrias **10**: 1–230, Karlsruhe.

Bernor, R.L., H. Tobien & M.O. Woodburne (1989): Patterns of Old World hipparionine evolutionary diversification and biogeographic extension. – In: Lindsay E.H., V. Fahlbusch & P. Mein (eds.): *Topics on European Mammalian Chronology*. Plenum: New York. pp. 263-319

Bernor, R .L., J. Kovar-Eder, D. Lipscomb, F. Rögl, S. Sen & H. Tobien (1988): Systematics, stratigraphic and paleoenvironmental contexts of first-appearing *Hipparion* in the Vienna Basin, Austria. – Journal of Vertebrate Paleontology **8**:427–452. Los Angeles.

Bernor, R.L., R.S. Scott, M. Fortelius, J. Kappelman, M. Armour-Chelu & S. Sen. (in prep): Systematics and Evolution of the Late Miocene Hipparions from Sinap, Turkey. - In: Fortelius, M., Kappelman, J., Sen, S. and Bernor, R.L. (eds.). The Sinap Formation. Columbia University Press.

Bolliger, T. (1996): A Current Understanding About the Anomalomyidae (Rodentia): Reflections on Stratigraphy, Paleobiogeography, and Evolution. – In: Bernor, R. L., V. Fahlbusch & H.-W. Mittmann (eds.): *The Evolution of Western Eurasian Neogene Mammal Faunas*. Columbia University Press: New York. pp. 235–245.

Bolliger, T. (1999): Family Anomalomyidae. – In: Rössner, G.E. & K. Heissig (eds.): The Miocene Land Mammals of Europe. Verlag Dr. Friedrich Pfeil: München. pp. 411–420.

Eisenmann, V. (1995): What metapodial morphometry has to say about some Miocene hipparions. – In: Paleoclimate and Evolution – With Emphasis on Human Origins; Yale: New Haven. pp. 148–163.

Eisenmann, V., M.-T. Alberdi, C. de Giuli & U. Staesche (1988): Studying Fossil Horses Volume I: Methodology. – In: Woodburne, M. O. & P.Y. Sondaar (eds.): Collected papers after the "New York International Hipparion Conference, 1981". Brill: Leiden. pp. 1–71.

Fahlbusch, V. (1991): The Meaning of MN-Zonation: Considerations for a Subdivision of the European Continental Tertiary Using Mammals. – Newsl. Stratigr. **24** (3): 159–173. Stuttgart.

Fortelius, M. & Solounias, N. (in press): Functional characterization of ungulate molars using abrasion attrition wear gradient. – American Museum Novitates.

Gabunia, L.K. (1959): Histoire du genre *Hipparion*. – Ed. Acad. Sci., USSR, Moscou, traduction en français B.R.G.M., 69 Fig., 151 Tab., 23 Pl.; Paris.

Getty, R. (1982): The Anatomy of Domestic Animals. 1211 pp. Philadelphia

Gromova, V. (1952): Le Genre *Hipparion*. – Institute de Paleontologie Academie de Sciences, l'USSR **36**. 12: 1–473, 54 Abb., 18 Tab., 13 Taf: Paris.

Haas, J., E. Jocha-Edelényi, L. Gidai, M. Kaiser, M. Kretzoi & J. Oravecz (1984): Sümeg és környékének földtani felépítése [Geology of Sumeg and its neighbourhood]. – Geol. Hung. ser. Geol. **20**: 1–353. Budapest.

Hayek, L.-A., Bernor, R.L., Solounias, N. & Steigerwald, P. (1992): Preliminary studies of Hipparionine horse diet as measured by tooth microwear. – Ann. Zool. Fennici **28**:187–200. Helsinki.

Hensel, R. (1860): Über *Hipparion mediterraneum*. – Abh. Königl. Akad. Wiss., 27–121. Berlin.

Hunter, J. P. & M. Fortelius (1994): Comparative occlusal morphology, facet development, and microwear in two sympatric species of *Listriodon* (Mammalia: Suidae) from the middle Miocene of western Anatolia (Turkey). – Journal of Vertebrate Paleontology **14**(1): 105–126. Los Angeles.

Jungers, W.L., A.B. Falsetti, & C.E. Wall (1995): Shape, relative size, and size-adjustments in morphometrics. – Yearbook of Physical Anthropology **38**: 137–161.

Kordos, L. (1987a): *Karstocricetus skofleki* gen.n., sp. n. and the evolution of the Late Neogene Cricetidae in the Carpathian Basin. – Frag. Min. et Pal. **13**: 65–88.

Kordos, L. (1987b): Neogene Vertebrate Biostratigraphy in Hungary. – Ann. Inst. Geol. Publ. Hung., **70**: 393-396.

Kordos, L. (1989): Anomalomyidae (Mammalia, Rodentia) Remains from the Neogene of Hungary. – Földt. Int. Évi Jel. 1987-röl. **1989**: 293-311.

Kordos, L. (1992): Magyarország harmad- és negyedidöszaki emlösfaunájának fejlödése és biokronológiája [Evolution and Biochronology of the Tertiary and Quaternary Mammal Fauna of Hungary]. – DSc Thesis, manuscript, Budapest.

Kordos, L., I. Meszaros, L. Magyar, P. Mueller & R.L. Bernor (in prep.): Recent paleontological results on the Tihany Section.

Koufos, G. D. (1984): A new hipparion (Mammalia, Perissodactyla) from the Vallesian (Late Miocene) of Greece. – Paläont. Z. **58**(3/4): 307–317. Stuttgart.

Koufos, G. D. (1987): Study of the Pikermi hipparions Part I: Generalities and taxonomy. – Bull. Mus. natn. Hist. nat., Paris, 4e sér., **9**, 1987 section C, n° 2: 197–252. Paris.

Kowalski, K. (1994): Evolution of *Anomalomys* GAILLARD, 1900 (Rodentia, Mammalia) in the Miocene of Poland. – Acta Zool. Cracoviensia 37(1): 163–176. Cracov.

Kretzoi, M. (1954): Rapport final des fouilles paléontologiques dans la grotte de Csákvár. – Földt. Int. Évi Jel. 1954: 55–68. Budapest.

Kretzoi, M. (1969): Sketch of the Late Cenozoic (Pliocene and Quaternary) Terrestrial Stratigraphy of Hungary. – Földrajzi Közlemények, 17(3): 198-204. Budapest.

Kretzoi, M. (1984): A Sümeg-Gerinci fauna és faunaszakasz [Fauna and faunal stage of Sümeg-Gerinc]. – Geol. Hung. ser. Geol. 20: 214–222. Budapest.

Kretzoi, M. (1987): Terrestrische Biochronologie/Stratigraphie des Karpatenbeckens im Pannonien (s.l.). – Ann. Hung. Geol. Inst. 69: 409–422. Budapest.

Kretzoi, M. & M. Pécsi (1982): Pliocene and Pleistocene Development and Chronology of the Pannonian Basin. – Föld. Közlem. 31(4): 300–326. Budapest.

Mein, P. (1975): Résultats du Groupe de Travail des Vertébrés. – In: Senes, J. (ed.): Report on Activity of R.C.M.N.S. Working Group. Reg. Comm. Med. Neogene Stratigraphy. p. 78–81.

Mein, P. (1979): Rapport d'activité du groupe de travail vertébré mise à jour de la biostratigraphie du neogène basée sur les mammifères. Ann. Géol. Pays Hellén. p. 1367–1372. Athens.

Mein, P. (1989): Updating of MN Zones. – In: Lindsay, E.H., F. Fahlbusch & P. Mein (eds.): *European Neogene Mammal Chronology*. Plenum: New York. p. 73–90.

Nickel, R., A. Schummer & E. Seiferle (1986): The Anatomy of the Domestic Animals 1. The Locomotor System of the Domestic Animals. 499 pp. Berlin & Hamburg.

Rabeder, G. (1985): Die Säugetiere des Pannonien. – In: Papp, A., Á. Jámbor & F.F. Steininger (eds.): *Chronostratigraphie und Neostratotypen, Miozan M6, Pannonien*, pp.440–463., Akadémiai Kiadó, Budapest.

Rensberger, J.M. (1978): Scanning electron microscopy of wear and occlusal events in some small herbivores. – In: P. M Butler & K.A. Joysey, (eds.): *Development, Function and Evolution of Teeth*. pp.415–438. Acad. Press: New York.

Rögl, F., H. Zapfe, R.L Bernor, R. Brzobohaty, G. Daxner-Höck, I. Draxler, O. Fejfar, J. Gaudat, P. Herrmann, G. Rabeder, O. Schultz & R. Zettler (1993): Die Primatenfundstelle Götzendorf an der Leitha (Obermiozän des Wiener Beckens, Niederösterreich). – Jb. Geol. B. – A. 136(2): 503–526. Wien.

Rögl, F. & G. Daxner-Höck (1996): Late Miocene Paratethys correlations.. – In: Bernor R.L., V. Fahlbusch & H.-W. Mittmann (eds.): *The Evolution of Western Eurasian Neogene Mammal Faunas*. Columbia University Press: New York. pp. 47–55

Schaub, S. & H. Zapfe (1953): Die Fauna der miozanen Spaltenfüllung von Neudorf an der March (CSR). – Öst. Akad. Wiss. math.-naturw. Kl. 163(3): 181–215. Wien.

Scott, K.M. (1990): Postcranial dimensions of ungulates as predictors of body mass. – In: Damuth, J., B.J. Macfadden (eds.): *Body Size in Mammalian Paleobiology: Estimation and Biological Implications*. Cambridge University Press: Cambridge. pp. 301–335.

Solounias, K. & L A.C. Hayek. (1988): Dietary adaptions and paleoecology of the late Miocene ruminants from Pikermi and Samos in Greece. – Palaeontogr. Palaeoclim. Palaeoecol. 65:159–172.

Solounias, N. & L.A. Hayek (1993): New methods of tooth microwear analysis and application to dietary determination of two extinct antelopes. – J. Zool., Lond. 229: 421–445.

Solounias, N. & S.M.C. Moelleken. (1992): Dietary adaptations of two goat ancestors and evolutionary considerations. – Géobios 25(6): 797–809.

Solounias, N. & S.M.C. Moelleken. (1993): Tooth microwear and premaxillary shape of an archaic antelope. – Lethaia 26: 261–268.

Solounias, N. & S.M.C. Moelleken. (1994): Differences in diet between two archaic ruminant species from Sansan, France. – Historical Biology 7: 203–220.

Solounias, N., M.F. Teaford, & A. Walker (1988): Interpreting the diet of extinct ruminants: the case of a non-browsing giraffid. – Paleobiology 14: 287–300.

Steininger, F.F., W.A. Berggren, D.V. Kent, R.L. Bernor, S. Sen & J. Agusti (1996): Circum-Mediterranean Neogene (Miocene and Pliocene) marine-continental chronologic correlations of European mammal units. - In: Bernor, R.L., V. Fahlbusch & H.W. Mittmann (eds.): *The Evolution of Western Eurasian Neogene Mammal Faunas*. Columbia University Press: New York. pp. 7–46.

Swisher, C.C. III (1996): New 40Ar/39Ar dates and their contribution toward a revised chronology for the late Miocene nonmarine of Europe and West Asia. – In: Bernor, R. L., V. Fahlbusch & H.-W. Mittmann (eds.): *The Evolution of Western Eurasian Neogene Mammal Faunas*. Columbia University Press: New York. pp. 64–77.

Teaford, M.F. (1991): Dental microwear: What can it tell us about diet and dental function? – In: M.A. Kelly & C. Spencer Larsen (eds.): Advances in dental anthropology. Wiley-Liss Inc.: New York. pp. 341–356.

Teaford, M. F. & A.C. Walker, (1983): Dental microwear in adult and still-borne guinea pigs (*Cavia porcellus*). – Arch. Oral Biol. **28**: 1077–1081.

Teaford, M.F. & A. Walker (1984): Quantitative differences in dental microwear between primate species with different diets and a comment on the presumed diet of *Sivapithecus*. – Am. J. Phys. Anthropol. **64**: 191–200.

Van Valkenburg, B. V., M. F. Teaford., & A. Walker. (1990): Molar microwear and diet in large carnivores: inference concerning diet in the sabretooth cat, *Smilodon fatalis*. – J. Zool. Lond. **222**: 319–340.

Woodburne, M. O., R. L. Bernor & C.C. Swisher III (1996): An appraisal of the stratigraphic and phylogenetic bases for the "Hipparion Datum" in the Old World. - In: Bernor, R.L., V. Fahlbusch & H.-W. Mittmann (eds.): *The Evolution of Western Eurasian Neogene Mammal Faunas*, Columbia University Press: New York. pp.124–136.

Woodburne, M. O., G. Theobald, R.L. Bernor, C.C. Swisher III, H. König & H. Tobien. (1996a): Advances in Geology and Stratigraphy at Höwenegg, Southwestern Germany. In: Bernor, R.L., V. Fahlbusch & H.-W. Mittmann (eds.): *The Evolution of Western Eurasian Neogene Mammal Faunas*, Columbia University Press: New York. pp.106–123.

Legend of Hipparionine Character States (following Bernor et al., 1989 and Bernor & Lipscomb 1991, 1995; Bernor & Armour-Chelu, 1999)

C1) Relationship of lacrimal to the preorbital fossa: A = lacrimal large, rectangularly shaped, invades medial wall and posterior aspect of preorbital fossa; B = lacrimal reduced in size, slightly invades or touches posterior border of preorbital fossa; C = preorbital bar (POB) long with the anterior edge of the lacrimal placed more than half the distance from the anterior orbital rim to the posterior rim of the fossa; D = POB reduced slightly in length but with the anterior edge of the lacrimal placed still more than 1/2 the distance from the anterior orbital rim to the posterior rim of the fossa; E = POB vestigial, but lacrimal as in D; F = POB absent; G = POB very long with anterior edge of lacrimal placed less than 1/2 the distance from the anterior orbital rim to the posterior rim of the fossa; H = POB absent.

C2) Nasolacrimal fossa: A = POF large, ovoid shape and separated by a distinct medially placed, dorsoventrally oriented ridge, dividing POF into equal anterior (nasomaxillary) and posterior (nasolacrimal) fossae; B = nasomaxillary fossa sharply reduced compared to nasolacrimal fossa; C = nasomaxillary fossa absent (lost), leaving only nasolacrimal portion (when a POF is present).

C3) Orbital surface of lacrimal bone: A = with foramen; B = reduced or lacking foramen.

C4) Preorbital fossa morphology: A = large, ovoid shape, anteroposteriorly oriented; B = POF truncated anteriorly; C = POF further truncated, dorsoventrally restricted at anterior limit; D = subtriangular shaped and anteroventrally oriented; E = subtriangularly shaped and anteroposteriorly oriented; F = egg-shaped and anteroposteriorly oriented; G = C-shaped and anteroposteriorly oriented; H = vestigial but with a C-shaped or egg-shaped outline; I = vestigial without C-shape outline, or absent; J = elongate, anteroposteriorly oriented; K = small, rounded structure; L = posterior rim straight, with non-oriented medial depression.

C5) Fossa posterior pocketing: A = deeply pocketed, greater than 15 mm in deepest place; B = pocketing reduced, moderate to slight depth, less than 15 mm; C = not pocketed but with a posterior rim; D = absent, no rim but a remnant depression; E = absent.

C6) Fossa medial depth: A = deep, greater than 15 mm. in deepest place; B = moderate depth, 10–15 mm in deepest place; C = shallow depth, less than 10 mm in deepest place; D = absent.

C7) Preorbital fossa medial wall morphology: A = without internal pits; B = with internal pits.
C8) Fossa peripheral border outline: A = strong, strongly delineated around entire periphery; B = moderately delineated around periphery; C = weakly defined around periphery; D = absent with a remnant depression; E = absent, no remnant depression.
C9) Anterior rim morphology: A = present; B = absent.
C10) Placement of infraorbital foramen: A = placed distinctly ventral to approximately 1/2 the distance between the preorbital fossa's anteriormost and posteriormost extent; B = inferior to, or encroaching upon anteroventral border of the preorbital fossa.
C11) Confluence of buccinator and canine fossae: A = present; B = absent, buccinator fossa is distinctly delimited.
C12) Buccinator fossa: A = not pocketed posteriorly; B = pocketed posteriorly.
C13) Caninus (= intermediate) fossa: A = absent; B = present.
C14) Malar fossa: A = absent; B = present.
C15) Nasal notch position: A = at posterior border of canine or slightly posterior to canine border; B = approximately half the distance between canine and P2; C = at or near the anterior border of P2; D = above P2; E = above P3; F = above P4; G = above M1; H = posterior to M1.
C16) Presence of dP1 (16U) or dp1 (16L): A = persistent and functional; B = reduced and non-functional; C = absent.
C17) Curvature of maxillary cheek teeth: A = very curved; B = moderately curved; C = straight.
C18) Maximum cheek tooth crown height: A = < 30 mm; B = 30–40 mm; C = 40–60 mm; D = 60–75 mm; E = 75+ maximum crown height.
C19) Maxillary cheek tooth fossette ornamentation: A = complex, with several deeply amplified plications; B = moderately complex with fewer, more shortly amplified, thinly banded plications; C = simple complexity with few, shortly amplified plications; D = generally no plis; E = very complex.
C20) Posterior wall of postfossette: A = may not be distinct; B = always distinct.
C21) Pli caballin morphology: A = double; B = single or occasionally poorly defined double; C = complex; D = plis not well formed.
C22) Hypoglyph: A = hypocone frequently encircled by hypoglyph; B = deeply incised, infrequently encircled hypocone; C = moderately deeply incised; D = shallowly incised.
C23) Protocone shape: A = round q-shape; B = oval q-shape; C = oval; D = elongate-oval; E = lingually flattened-labially rounded; F = compressed or ovate; G = rounded; H = triangular; I = triangular-elongate; J = lenticular; K = triangular with rounded corners.
C24) Isolation of protocone: A = connected to protoloph; B = isolated from protoloph.
C25) Protoconal spur: A = elongate, strongly present; B = reduced, but usually present; C = very rare to absent.
C26) Premolar protocone/hypocone alignment: A = anteroposteriorly aligned; B = protocone more lingually placed.
C27) Molar protocone/hypocone alignment: A = anteroposteriorly aligned; B = protocone more lingually placed.
C28) P2 anterostyle (28U) / paraconid (28L): A = elongate; B = short and rounded.
C29) Mandibular incisor morphology: A = not grooved; B = grooved.
C30) Mandibular incisor curvature: A = curved; B = straight.
C31) I3 lateral aspect: A = elongate, not labiolingually constricted; B = very elongate, labiolingually constricted distally; C = atrophied.
C32) Premolar metaconid: A = rounded; B = elongated; C = angular on distal surface; D = irregular shaped; E = square shaped; F = pointed.
C33) Molar metaconid: A = rounded; B = elongated; C = angular on distal surface; D = irregular shaped; E = square shaped; F = pointed.
C34) Premolar metastylid: A = rounded; B = elongate; C = angular on proximal surface; D = irregular shaped; E = square shaped; F = pointed.
C35) Premolar metastylid spur: A = present; B = absent
C36) Molar metastylid: A = rounded; B = elongate; C = angular on proximal surface; D = irregular shaped; E = square shaped; F = pointed.
C37) Molar metastylid spur: A = present; B = absent

C38) Premolar ectoflexid: A = does not separate metaconid and metastylid; B = separates metaconid and metastylid.
C39) Molar ectoflexid: A = does not separate metaconid and metastylid; B = separates metaconid and metastylid; C = converges with preflexid and postflexid to abutt against metaconid and metastylid.
C40) Pli caballinid: A = complex; B = rudimentary or single; C = absent.
C41) Protostylid: A = present on occlusal surface often as an enclosed enamel ring; B = absent on occlusal surface, but may be on side of crown buried in cement; C = strong, columnar; D = a loop; E = a small, poorly developed loop; F = a small, pointed projection continuous with the buccal cingulum.
C42) Protostylid orientation: A = courses obliquely to anterior surface of tooth; B = less oblique coursing, placed on anterior surface of tooth; C = vertically placed, lies flush with protoconid enamel band; D = vertically placed, lying lateral to protoconid band; E = open loop extending posterolabially.
C43) Ectostylids: A = present; B = absent.
C44) Premolar linguaflexid: A = shallow; B = deeper, V-shaped; C = shallow U-shaped; D = deep, broad U-shape; E = very broad and deep.
C45) Molar linguaflexid: A = shallow; B = V-shaped; C = shallow U-shaped; D = deep, broad U-shape; E = very broad and deep.
C46) Preflexid morphology: A = simple margins; B = complex margins; C = very complex.
C47) Postflexid morphology: A = simple margins; B = complex margins; C = very complex.
C48) Postflexid invades metaconid/metastylid junction by anteriormost portion bending sharply lingually: A = no; B = yes.
C49) Protoconid enamel band morphology: A = rounded; B = flattened.